

EUR 4238 e

EUROPEAN ATOMIC ENERGY COMMUNITY - EURATOM

LIBRARY

**PROGRAM FOR PLUTONIUM UTILIZATION
IN THERMAL REACTORS**

1969



Report prepared by ENEL
Ente Nazionale per l'Energia Elettrica - Rome, Italy

Euratom Contract No. 092-66-6 TEEI

LEGAL NOTICE

This document was prepared under the sponsorship of the Commission of the European Communities.

Neither the Commission of the European Communities, its contractors nor any person acting on their behalf :

make any warranty or representation, express or implied, with respect to the accuracy, completeness, or usefulness of the information contained in this document, or that the use of any information, apparatus, method, or process disclosed in this document may not infringe privately owned rights; or

assume any liability with respect to the use of, or for damages resulting from the use of any information, apparatus, method or process disclosed in this document.

This report is on sale at the addresses listed on cover page 4

at the price of FF 10.—	FB 100.—	DM 8.—	Lit. 1 250	Fl. 7.25
-------------------------	----------	--------	------------	----------

When ordering, please quote the EUR number and the title, which are indicated on the cover of each report.

Printed by Guyot, s.a.
Brussels, August 1969

This document was reproduced on the basis of the best available copy.

EUR 4238 e

EUROPEAN ATOMIC ENERGY COMMUNITY - EURATOM

PROGRAM FOR PLUTONIUM UTILIZATION IN THERMAL REACTORS

1969



Report prepared by ENEL
Ente Nazionale per l'Energia Elettrica - Rome, Italy

Euratom Contract No. 092-66-6 TEEI

ABSTRACT

The contract is articulated in eight technical tasks and one for coordination; during this reporting period, no work was performed on Task V, whilst Task I was terminated during the first year of implementation.

TASK II : Development of a calculation method for Pu lattices

Several computer codes (FLARE, TURBO, RIBOT, BURNY, GAM-THERMOS-SQUID) were further developed and checked against experimental data from DIMPLE, SAXTON and PRCF critical measurements.

TASK III : Minimum critical load with Pu prototype elements

The minimum critical loads with U and Pu fuel elements were calculated. The optimal configuration of a 3×3 core for power distribution measurements was determined. The gamma-scan equipment to be used for these measurements was thoroughly checked out.

TASK IV : Isotopic composition measurements on irradiated uranium fuel

Preparation for these measurements at the European Institute for Trans-uranium Elements at Karlsruhe is in progress.

TASK VI : Detailed study of Pu fuel cycles

12 prototype Pu bearing fuel bundles are to be loaded into the Garigliano core at the beginning fuel cycle No. 2. The optimal positioning, the power distribution and the reactivity life have been determined.

TASK VII : Reactor safety analysis, plant behaviour during operating transients and accidents

Work under this task was limited to the health physics problems associated with Pu fuel handling.

TASK VIII : Conceptual mechanical design of the fuel element and technical specifications for fuel procurement

A meeting with the Community manufacturers on the problems associated with the fabrication of a second series of Pu prototype elements was held in Brussels on September 19-21, 1967.

KEYWORDS

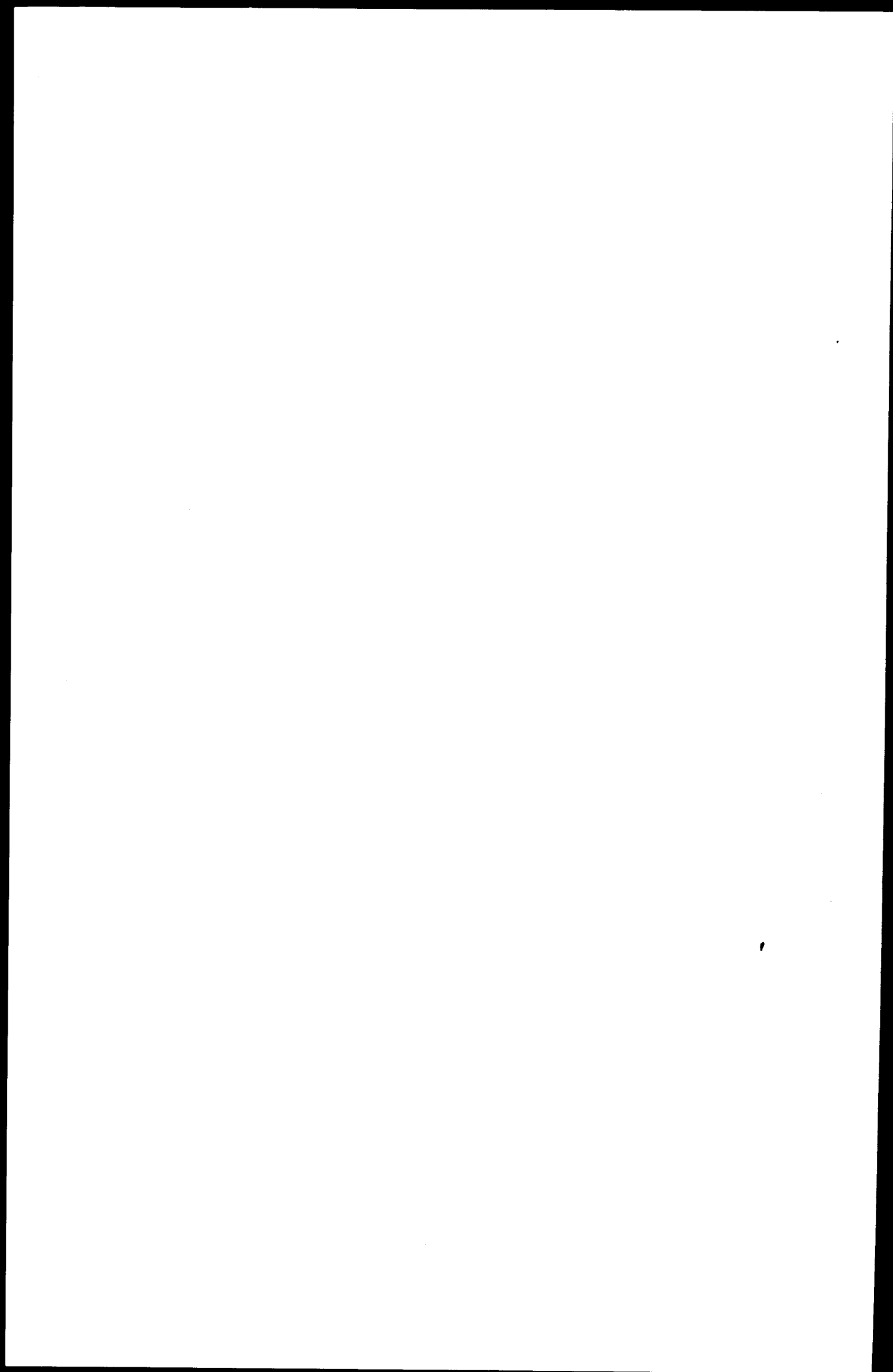
PLUTONIUM
THERMAL NEUTRONS
REACTORS
FUEL ELEMENTS
SENN-1

I N D E X

	Page
INTRODUCTION	7
TASK II - DEVELOPMENT OF A CALCULATION METHOD FOR PLUTONIUM LATTICES	8
1. Development and verification of calculation methods for mixed uranium and plutonium lattices	8
2. Development and modification of the codes used for the research program	II
FLARE code	II
AGENA code	II
BURNY code	II
BURNY-2 code	II
RIBOT-5-SQUID code system	II
TASK III - MINIMUM CRITICAL LOAD WITH PLUTONIUM PROTOTYPE ELEMENTS	12
1. Determination of the minimum critical loads and selec- tion of the 3x3 configuration for power distribution measurements	12
1.1 Evaluation of the perturbation induced by a bank of control rods on the radial power distribution	12
1.2 Determination of the minimum critical load for enriched-uranium and plutonium elements	14
1.3 3x3 assembly for power distribution measurements	18
2. Preliminary measurements for the development of a gamma scanning technique for plutonium fuel rods	22
2.1 Description of the equipment	26
2.2 Measurements	26
2.3 Gamma measurements	33
2.4 Difficulties encountered during the measurements	36
2.5 Test results	37
2.5.1 Radiation levels	37
2.5.2 Gamma spectrometry	37

	Page
2.6 Analysis of the results	37
2.6.1 Gross gamma measurements	37
2.6.2 La-140 measurement	42
2.6.3 Relationship between the two counting chains	43
2.6.4 Determination of the radiation levels	43
2.7 Conclusions	45
2.8 Proposed procedure for the measurements during the refueling outage	45
 TASK IV - ISOTOPIC COMPOSITION MEASUREMENTS ON IRRADIATED URANIUM FUEL	 47
1. Schedule of tests to be performed on rods of element A-106	47
2. Problems associated with transport of irradiated fuel rods to the Karlsruhe Center	49
 TASK VI - DETAILED STUDY OF PLUTONIUM FUEL CYCLES	 50
1. Analysis for the positioning of plutonium elements in the Garigliano core at the beginning of cycle 2	50
2. Characteristics of the reload fuel elements	50
3. Reload uranium element	52
4. Prototype standard plutonium elements	52
5. Prototype advanced plutonium elements	52
6. Preliminary determination of the core burn-up distribution at the end of Cycle 1C	52
7. Preparation of the library for the FLARE code	57
8. Positioning of prototype plutonium elements	61
9. Analysis of the perturbations in the local power distribution caused by lack of one rod in the reload fuel elements	61

	Page
TASK VII - REACTOR SAFETY ANALYSIS, PLANT BEHAVIOUR DURING OPERATING TRANSIENTS AND ACCIDENTS	70
TASK VIII - CONCEPTUAL MECHANICAL DESIGN OF THE FUEL ELEMENT AND TECHNICAL SPECIFICATIONS FOR FUEL PROCUREMENT	72
LIST OF REPORT ISSUED DURING THE SECOND YEAR OF IMPLEMENTATION OF THE ENEL EURATOM CONTRACT 092-66-6-TEEI	73



PROGRAM FOR PLUTONIUM UTILIZATION IN THERMAL REACTORS

INTRODUCTION (*)

This report contains the main results of the work carried out under the ENEL-EURATOM contract, No. 092-66-6-TEEI, during the second year of implementation.

The contract is articulated in eight technical tasks and one for coordination; during this reporting period, no work was performed on Task V, whilst Task I was terminated during the first year of implementation. Therefore, these tasks have been omitted in this report.

In addition to a summary description of the work performed and under way for each task, the report describes the twelve prototype plutonium fuel elements that will be inserted in the Garigliano reactor during the first refueling shutdown scheduled for the summer of 1968. Eight of these elements are made entirely of plutonium and are called "standard", whereas the other four contain both enriched-uranium and mixed uranium-plutonium rods and are called "advanced".

In this reporting year, ENEL and EURATOM jointly decided to issue an invitation to bid for a second set of prototype plutonium elements to be supplied by a Community manufacturer for insertion in the Garigliano reactor during the refueling shutdown scheduled for the end of 1969.

A list of documents issued between 1 June 1967 and 31 May 1968 -- available at the EURATOM offices -- is attached.

(*) Manuscript received on 25 November 1968.

TASK II - DEVELOPMENT OF A CALCULATION METHOD FOR PLUTONIUM LATTICES

The work under this task consisted essentially in developing codes and calculation procedures to use in the research program. The procedures followed for the calculation of power distribution from experimental data are discussed in a separate topical report, "Development and Verification of Calculation Methods for Mixed Uranium and Plutonium Lattices", Doc. 4.811/12. The more important of the results obtained with these procedures are illustrated below.

The preparation of the codes necessitated the compilation of several programs and their adaptation to the IBM 360/65 at the Common Research Center at Ispra.

1. Development and verification of calculation methods for mixed uranium and plutonium lattices

The power distribution calculation methods used for the work under this research program were subjected to extensive investigation aiming at ascertaining their adequacy in handling the various aspects of UO_2 and UO_2 - PuO_2 cores.

Two categories of codes can be envisaged for this purpose:

- (a) Codes which permit the determination of the macroscopic power distribution of the whole core as a function of irradiation.
- (b) Codes which permit the assessment of the effect of local disuniformities on power distribution over the fuel lifetime.

For the determination of the macroscopic power distribution in BWR's, the FLARE code was chosen because of its flexibility and economic advantages. A TURBO type code (CONDOR) appeared more suited to PWR problems; the microscopic library was generated by means of the RIBOT code.

For the second task, use was made of the BURNY code in the two-group and five-group (two thermal and three fast) versions. These versions were checked against experimental data to assess the increased accuracy attainable from a more detailed representation of the neutron spectrum, and against experimental distributions of U-235 and Pu-239 fission rates to ascertain their capability of representing the variation in the fissile isotope content with irradiation.

The survey was also extended to the three-group (one thermal and two fast) GAM-THERMOS-SQUID system; the thermal constants of the peripheral cells of elements were calculated by THERMOS on the basis of a slab model of the fuel cell and adjacent water gap.

The experimental data utilized to trim and verify the FLARE code were the operating data and the results of three gamma scans carried

out at the Garigliano EWR station during the first two operating cycles. The experimental data utilized for the CONDOR code were constituted of Aeroball measurements carried out at the Trino PWR station. The calculated data compare favourably with the experimental ones.

The local power distribution codes were verified against the following experimental data:

- (1) DIMPLE measurements, performed by UKAEA for ENEL, of U-235 and Pu-239 fission rates; by means of foils on four different 5x5 arrays of fuel modules, each module containing 8x8 Al-canned pins. Rod pitch and gap between modules closely resembled those of the twelve plutonium fuel elements to be loaded in the Garigliano reactor. Array 1: all uranium-enriched (3%) modules. Array 2: as Array 1, except for plutonium-enriched (2.1%) central module. Array 3: as Array 2, except that the four corner pins of the central module had lower enrichment (1.2% Pu). Array 4: as Array 1, except that the plutonium module was loaded at the periphery.
- (2) Saxton plutonium program data. These data constitute a valid check because they provide the power perturbations due to water-gap and power sharing effects in cores of high plutonium content.
- (3) PRCF 1967 data from Battelle. These data were very interesting for the checks, as they were obtained on plutonium fuels with substantially different isotopic compositions.

The comparison results summarized in Table 1 indicated that:

(a) the one-thermal-group technique generally gives better agreement with the actual power distribution; (b) the corner rod power is slightly overestimated by the two-thermal-group technique and underestimated by the one-group technique; (c) the Pu-239 and U-235 fission rate ratios are evaluated better by the two-thermal-group technique; (d) the GAM-THERMOS-SQUID system shows that the allowances for the spectrum softening due to the water gap permit the one-thermal-group technique to achieve the same accuracy as the two-thermal group system; however, the GAM-THERMOS-SQUID technique is very time-consuming.

For flexibility and simplicity in use, codes which calculate the constants automatically by a fitting procedure, such as BURNBY, are very convenient for power distribution calculations also in the two-group version. For calculations over the fuel lifetime the five-group version (two thermal) appears to be more precise.

A further check will be provided by the performance of the plutonium elements at the Garigliano.

TABLE 1

		Power distribution, σ_{\pm} (%)			Fission rate ratio, σ_{\pm} (%)			$(K_{eff})_{theor.} - (K_{eff})_{exp.}$		
		Burny 2	Burny 5	G-TH-S	Burny 2	Burny 5	G-TH-S	Burny 2	Burny 5	G-TH-S
A	Array 1	1.4	2.5	-	-	-	-	+0.0117	-0.0012	-
	Array 2	1.4	2.8	4.2	7.6	2.3	2.3	+0.0075	-0.0015	-0.0101
	Array 3	1.1	1.7	-	7.7	1.9	-	+0.0065	-0.0026	-
	Array 4	3.2	2.2	-	9.3	2.8	-	+0.0164	+0.0073	-
B	6 Arrays	0.8-1.4	1.8-2.0	-	-	-	-	+0.0094 to +0.0180	-0.0053 to +0.0073	-
C	2 Arrays	1.6;3.4	-	-	-	-	-	+0.0089; +0.0170	-	-

A = DIMPLE REACTOR

B = SAXTON PROGRAMME

C = P R C F

2. Development and modification of the codes used for the research program

FLARE code

To improve the FLARE code as a calculation tool, it was translated from the FORTRAN II to FORTRAN IV language so that it could be used with an IBM 360/65. At the same time, a sub-routine was developed to enable the FLARE code to use Haling's technique which determines the optimum power distribution over an entire irradiation phase on the basis of the operating conditions at the end of that phase. In addition, the number of nodes was increased from $12 \times 12 \times 8$ to $16 \times 16 \times 16$, which thus permits a more accurate representation of local conditions in the core, especially in the axial direction.

AGENA code

Like FLARE, this code for fuel cycle cost calculations was translated from FORTRAN II into FORTRAN IV for use with the IBM 360/65.

RIBOT code

The translation of this code, which is a point burnup code, into FORTRAN IV language was rather painstaking as several variables had to be transformed from single to double precision because the first results were not quite in agreement with those obtained with the FORTRAN II code. This inconvenience was due to the fact that the data are represented with a slightly smaller number of significant digits in the processor of the IBM 360 than in that of the IBM 7090, and at times, especially in the case of differences between almost identical data, the result loses precision.

BURNY-2 code

This code was also fitted for use with the IBM 360/65 computer.

RIBOT-5-SQUID code system

Work is under way to link the 5-group RIBOT and SQUID codes. This burnup code system, which can be used in both the five-group (two thermal + three fast) and two-group (one thermal + one fast) versions, permits the solution of problems having a larger number of points, components and geometries and thus affords an analytical tool by far superior to the BURNY-2 code. At any rate, the latter is still an excellent means to solve optimization problems, thanks to its flexibility and low time consumption. The RIBOT-5-SQUID system, however, is still the most suited to represent the relationship between U-235 and Pu-239 reaction rates in $\text{UO}_2 + \text{PuO}_2$ lattices.

TASK III - MINIMUM CRITICAL LOAD WITH PLUTONIUM PROTOTYPE ELEMENTS

The work performed under this task consisted in determining the minimum critical loads and in selecting the 3x3 configuration with uranium and plutonium elements on which to perform the power distribution measurements. In addition, preliminary measurements on short fuel pins were performed at the station to perfect the technique for gamma scanning on individual plutonium rods.

1. Determination of the minimum critical loads and selection of the 3x3 configuration for power distribution measurements

For this purpose it was necessary to perform a number of calculations to evaluate the reactivity involved and the related power distribution. One of the criteria that were to be met in setting up the 3x3 configuration was that criticality was to be reached with the control rods inserted the least possible so that they would not affect the power distribution measurements. This condition can be met by replacing a certain number of Zr channels with SS channels, thus rendering the 3x3 assembly just slightly overcritical.

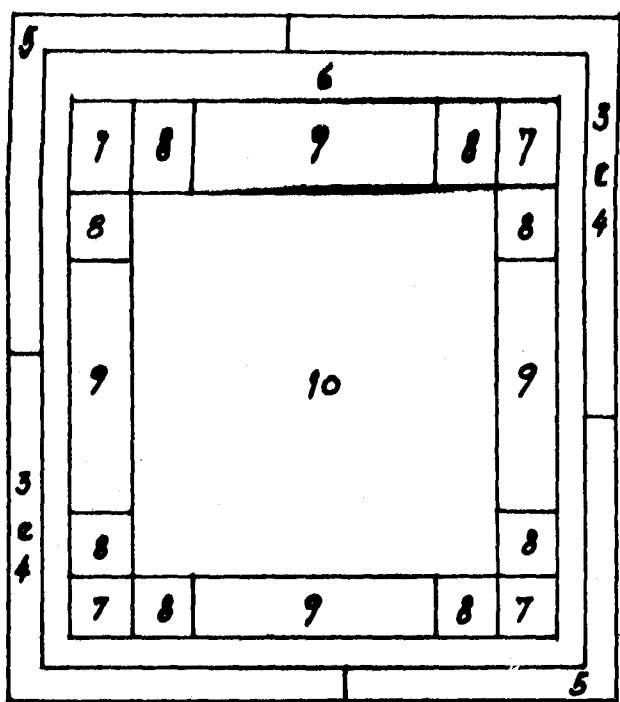
An analysis was also conducted to find the relationship between control rod insertion, absorbed reactivity and level at which the induced perturbation of the radial power distribution becomes negligible. This analysis gives a rough idea of the maximum overcriticality of the 3x3 assembly which the rods can control, while meeting the condition set above.

1.1 Evaluation of the perturbation induced by a bank of control rods on the radial power distribution

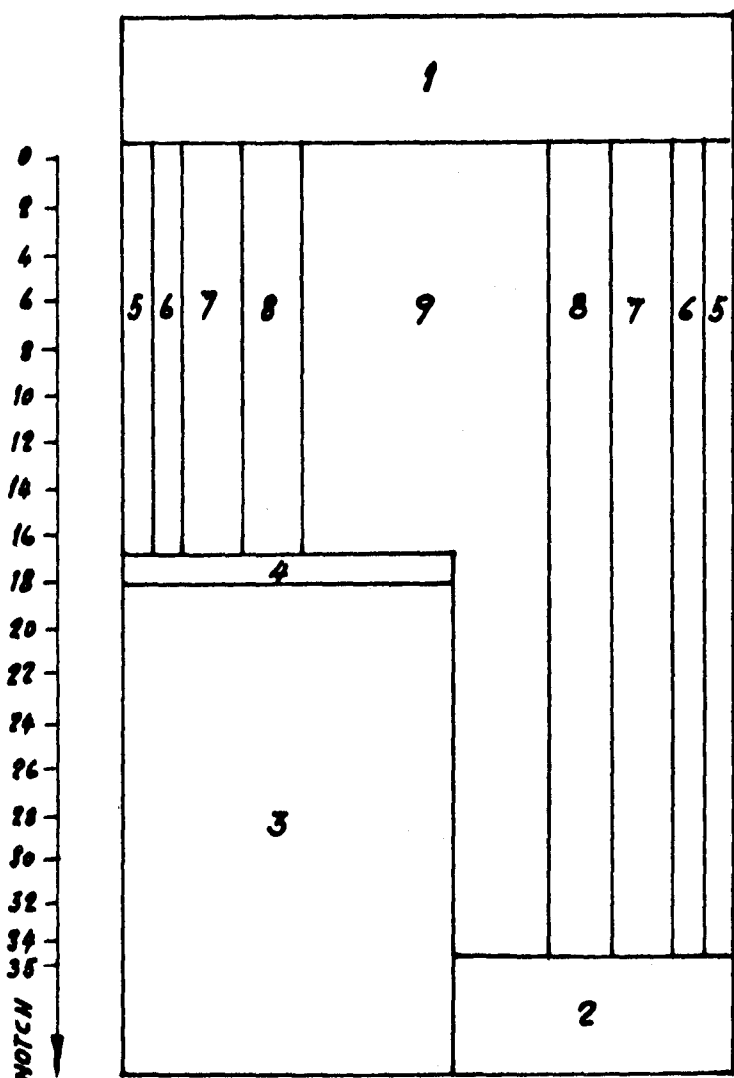
To evaluate the perturbation caused in the radial power distribution of a 3x3 assembly by a bank of control rods, use was made of a three-dimension diffusion code (TRITON). For application to reactivity and axial power distribution measurements, this code was verified by means of a one-dimension calculation with the FOG code applied to a typical channel. The results of the two calculations showed excellent agreement.

In view of the limitation of the TRITON code, it was necessary to exploit the characteristic modular nature of a core affected by bank insertion of all the control rods. Under these conditions it is possible to isolate a fuel element having partially inserted control rods at two of its corners.

The calculation was performed for the 2.3% enriched-uranium element with the control rods inserted midway (18th notch). The model used is shown in Fig. 3.1.



Schematization on the horizontal plane



REGIONS

1. Upper reflector
2. Lower reflector
3. Control rod
4. SS rod handle
5. Water gap
6. Zr Channel and adjacent water gap
7. Corner rod ($U_5 = 1.83\%$)
8. Peripheral rod ($U_5 = 1.83\%$)
9. Peripheral rod ($U_5 = 2.41\%$)
10. Inner rod ($U_5 = 2.41\%$)

Schematization on the vertical plane

FIG.3-1- MODEL USED FOR THE EVALUATION OF THE PERTURBATION INDUCED BY CONTROL ROD

In comparing the axial power distribution in position A (nearest the control rods) with that in position B (Fig. 3.2), the curves appear to nearly coincide at about 15 cm from the rod insertion height (from the top of the control rods). The local power distribution of the fuel element at this level is compared with that of an uncontrolled element in Fig. 3.3. The maximum deviation is found to be 2%.

At greater distances the deviation becomes negligible; so, it seems reasonable to conclude that a distance over 30 cm is sufficient to offset the perturbation. This is true also for other insertion levels, as in the conditions of interest (20°C) the characteristics of the moderator are axially uniform. A confirmation was provided by a calculation performed for the control rods positioned on the 28th notch.

The reactivity absorbed by the control rod bank, at the two insertion levels, was:

18th notch	1.41 Δ K/K%
28th notch	0.24 Δ K/K%

On the basis of the foregoing considerations and of the fact that the gamma scanning equipment does not permit the upper 50 cm of fuel rod to be monitored, it may be concluded that the control rod bank is not to exceed 2/3 of total insertion. This means that the 3x3 assembly must be supercritical by 2.5% at the most.

1.2 Determination of the minimum critical load for enriched-uranium and plutonium elements

The purpose of these experiments is to evaluate the accuracy with which the calculation method determines K_{∞} of plutonium elements. In order to obtain meaningful data for this assessment, it would be advisable to have two configurations, one of enriched-uranium elements and the other of plutonium elements. Thus, through a comparison with the results obtained for the enriched uranium it would be possible to determine the order of approximation which the calculation methods gives for plutonium elements.

In critical assemblies of these dimensions, radial neutron leakage is very high and any errors in their evaluation may compensate for errors in the K_{∞} . As a result, it is necessary to form the two minimum critical loads with the same number of elements and the same geometry so as to assume, with a fair degree of approximation, that the errors on neutron leakage are the same in both cases.

With the detailed calculation code, RIBOT-SQUID, the limits of which are described under Task II, two sets of calculations were carried out to determine the minimum critical load respectively for 2.3% enriched uranium elements and for standard plutonium elements. The calculations were performed in sequence, starting from an assembly of two elements, to which an element at a time was added. Fig. 3.4 shows the variation of

Uncontrolled region

SS
Handle

Controlled region

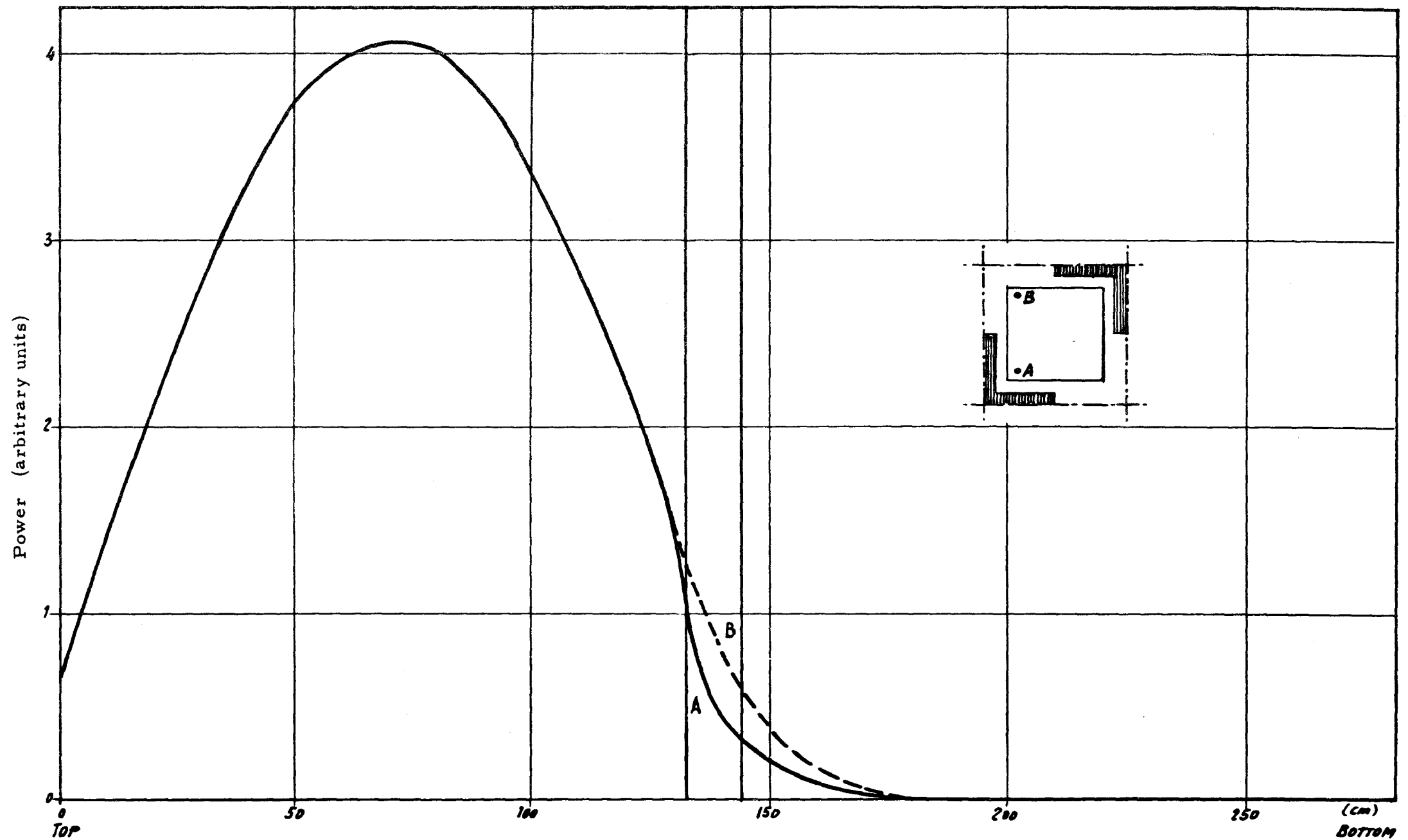


FIG. 3 - 2 - COMPARISON BETWEEN AXIAL POWER DISTRIBUTIONS IN THE TWO CORNER RODS

x	Non-perturbed values
xx	Values at 15 cm from the rods
xxx	Percentage difference between the two values

1.221							
1.197							
- 2.0							
1.195	0.972						
1.099	0.964						
- 1.5	- 0.9						
1.130	0.933	0.866					
1.120	0.931	0.857					
- 0.7	- 0.3	- 1.1					
1.134	0.911	0.838	0.813				
1.129	0.912	0.842	0.819				
- 0.5	+ 0.1	+ 0.4	+ 0.7				
1.134	0.911	0.838	0.813	0.813			
1.134	0.915	0.844	0.819	0.819			
0	+ 0.4	+ 0.7	+ 0.7	+ 0.7			
1.130	0.933	0.866	0.838	0.838	0.866		
1.137	0.940	0.872	0.844	0.842	0.857		
+ 0.6	+ 0.7	+ 0.6	+ 0.7	+ 0.4	- 1.1		
1.195	0.972	0.933	0.911	0.911	0.933	0.972	
1.126	0.981	0.940	0.916	0.912	0.931	0.964	
+ 0.9	+ 0.9	+ 0.7	+ 0.4	+ 0.1	- 0.3	- 0.9	
1.221	1.115	1.180	1.134	1.134	1.180	1.195	1.221
1.235	1.126	1.137	1.134	1.129	1.120	1.099	1.197
+ 1.1	+ 0.9	+ 0.6	0	- 0.5	- 0.9	- 1.5	- 2.0

FIG. 3-3 - COMPARISON BETWEEN POWER DISTRIBUTION OF CONTROLLED AND UNCONTROLLED FUEL ASSEMBLIES

K_{eff}

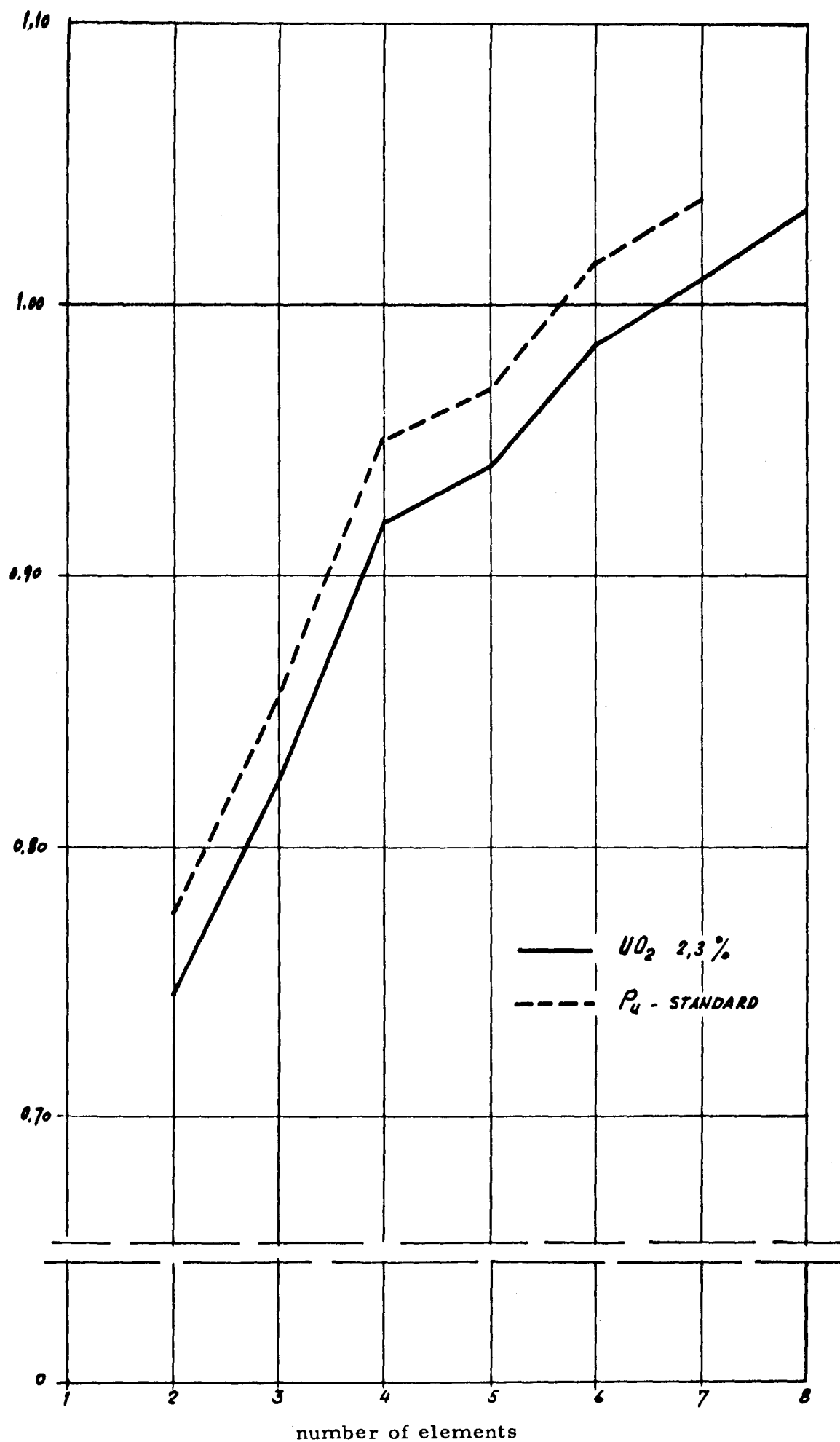


Fig. 3-4 - K_{eff} NUMBER OF ELEMENTS FOR THE ATTAINMENT OF CRITICALITY CONDITIONS

K_{eff} as a function of the number of elements for both types of fuel. Figures 3.5 and 3.6 give the corresponding bundle power distributions.

As well be noted in Fig. 3.4, the forecast indicates that critical conditions will be reached with a different minimum number of elements, that is, six for the plutonium fuel and seven for the uranium. To satisfy the condition formulated previously, the plutonium fuel assembly should contain seven elements. Fig. 3.4 also shows that an assembly of this size would be supercritical by about 4%.

On the other hand, in view of the uncertainty in the evaluation of the excess reactivity of an assembly through control rod calibration, it is advisable not to exceed a certain supercriticality value (less than 2%). For this reason, it is deemed preferable to set up a uranium assembly containing a few plutonium elements, in the same geometry of the uranium minimum critical load.

Reactivity calculations were performed for the two mixed configurations shown in Fig. 3.7, comprising respectively two and three plutonium elements. The expected K_{eff} values for these two configurations are 1.0254 and 1.0174 respectively, which are quite acceptable for the purpose of the measurements. If the expected figures should turn out to be incorrect and the criticality of the uranium assembly should require other than seven elements, the final size of the plutonium assembly will be selected on the basis of the information available at that time.

1.3 3x3 assembly for power distribution measurements

In selecting the configuration of the 3x3 assembly for power distribution measurements of the individual elements, the following criteria were adopted.

a) Limitation of supercriticality

As stated in the previous paragraph, control rods cause perturbation in the radial power distribution within 30 cm from their tips. So, for these measurements it is necessary to contain the supercriticality within limited values (below 2.5%) so that excessive rod insertion will not be required. The use of SS instead of Zr channels will help meet this condition.

b) A sufficiently flattened radial power distribution.

For measurement of local power peaks inside the fuel elements, it is well to have as flat a power distribution as possible; this can be achieved by proper positioning of the different elements and an appropriate use of SS channels.

c) High degree of symmetry.

To evaluate experimental deviations, it is useful to position the elements of the assembly considered so as to have lines of symmetry along the two diagonals and main axes.

0,862	1,276	0,862
0,862	1,276	0,862

6 ELEMENTS
 $K_{eff} = 0,9853$

	0,657	
0,765	1,483	0,955
0,844	1,261	0,844

7 ELEMENTS
 $K_{eff} = 1,0092$

	0,892	0,744
0,892	1,557	1,170
0,744	1,170	0,831

8 ELEMENTS
 $K_{eff} = 1,0339$

FIG. 3-5 - SEQUENCE FOR POWER DISTRIBUTION IN URANIUM ELEMENTS

0,995	1,125	
1,026	1,245	0,608

5 ELEMENTS

Keff = 0,9695

0,863	1,275	0,863
0,863	1,275	0,863

6 ELEMENTS

Keff = 1,0153

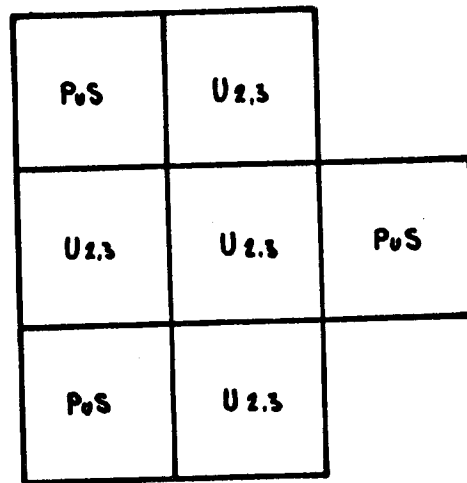
	0,661	
0,956	1,478	0,956
0,845	1,259	0,845

7 ELEMENTS

Keff = 1,0386

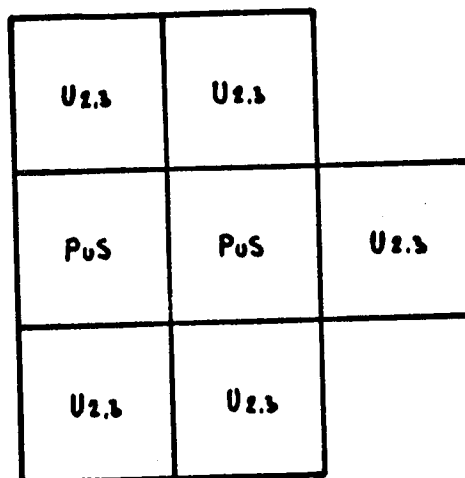
FIG. 3-6 - SEQUENCE FOR POWER DISTRIBUTION IN PLUTONIUM ELEMENTS

a)



$K_{eff} = 1.0174$

b)



$K_{eff} = 1.0254$

FIG. 3-7 - MINIMUM CRITICAL ARRAYS OF URANIUM AND PLUTONIUM ELEMENTS

- d) Presence in one octant of the three types of fuel elements (2.3% enriched uranium, standard plutonium and advanced plutonium). For practical reasons, the measurements will be limited to three elements, one for each type, and they will have to be located in the same octant so that the study may be carried out on a compact region.
- e) Proximity of uranium elements to standard plutonium elements. This condition will permit the theoretical assessment of the power sharing effect to be checked.

Fig. 3.8 shows the three selected configurations meeting the above-listed criteria. The detailed calculations were performed with the RIBOT-5-SQUID code and the K_{eff} obtained for configuration a) -- which is the best from the standpoint of power distribution -- was 1.0068. Since this figure is on the same order of magnitude as the error to which the calculation method is subject (0.7%) the calculations were repeated also on the other two configurations b) and c), which gave respectively 1.0257 and 1.0310.

In Figs 3.9 and 3.10 the calculated power distributions for the three configurations refer respectively to one of the main axes and the diagonal.

The rod power distributions will be calculated on the basis of the actual plutonium contents in each rod, of the position and actual orientation of the fuel elements. Data on this point are still being collected. A verification of the shutdown margin was performed on configuration a) of Fig. 3.8. The reactivity was found to be 0.82 with all rods in, and 0.92 with the highest-worth rod out. These margins are so wide that it was not considered worth while to extend the verification to configurations b) and c).

2. Preliminary measurements for the development of a gamma scanning technique for plutonium fuel rods

The purpose of these measurements was to:

- a) Test the equipment
- b) Determine how the fission product gamma spectra varied with time
- c) Establish the counting and data processing techniques
- d) Determine exposure and decay times, neutron flux levels, and the doses received by the personnel handling the elements.

For the measurements, six short pins were procured with the following isotopic compositions:

- two with a fissile Pu content of 0.74% (Pu - Type A)
- two with a fissile Pu content of 2.855% (Pu - Type C)
- two with uranium enriched to 2.4% (U).

a)

PuA	U _{2.3}	PuA
U _{2.3}	PuS	U _{2.3}
PuA	U _{2.3}	PuA

$K_{eff} = 1,0068$

b)

PuA	U _{2.3}	PuA
U _{2.3}	PuS	U _{2.3}
PuA	U _{2.3}	PuA

$K_{eff} = 1,0257$

c)

U _{2.3}	PuA	U _{2.3}
PuA	PuS	PuA
U _{2.3}	PuA	U _{2.3}

$K_{eff} = 1,0310$

— SS channel

— Zr channel

FIG. 3-8 - 3x3 ARRAY FOR POWER DISTRIBUTION MEASUREMENTS

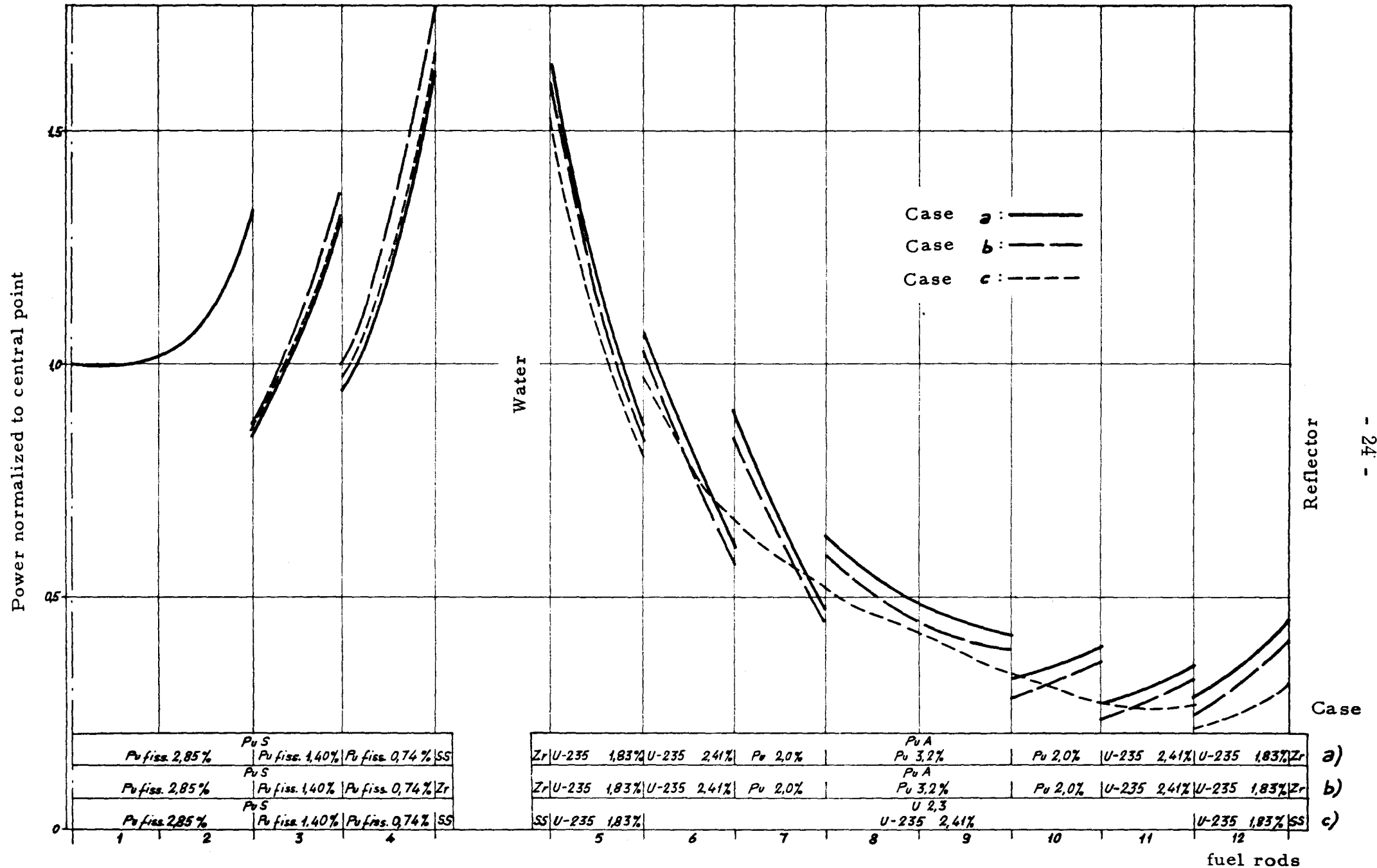


FIG. 3-10 - POWER DISTRIBUTION CALCULATED ALONG THE
DIAGONAL FOR THE 3x3 ARRAY

These pins were approximately 15 cm long and had the same structural characteristics of the normal plutonium and enriched-uranium fuel rods as shown in Fig. 3.11.

2.1 Description of the equipment

The test equipment is the same as will be used on the actual elements and it consists of three main parts:

- a) Rod movement and positioning mechanism
- b) Shield and detector system
- c) Detector pulse analyzing system.

Figs 3.12 and 3.13 show the rod positioning mechanism; Figs 3.14 and 3.15 show the shield and detector system. This equipment has all been installed in the fresh fuel vault.

The pulse analyzing system comprises two 400-channel analyzers of Laben make, complete with multiscaler and printer. The print-out system for the two analyzers differs in that one (chain 1) is very fast (400 channels in one minute) and operates in parallel, whereas the other (chain 2) has a lower printing speed (400 channels in 16 minutes) and operates in series. Because of this, a different measurement technique has been adopted: in chain 1 each spectrum is printed before integration, whereas chain 2 is used only for integration of the spectra and print-out of the integrals.

All the instruments are located on a walkway at about 4 meters above ground (Fig. 3.16).

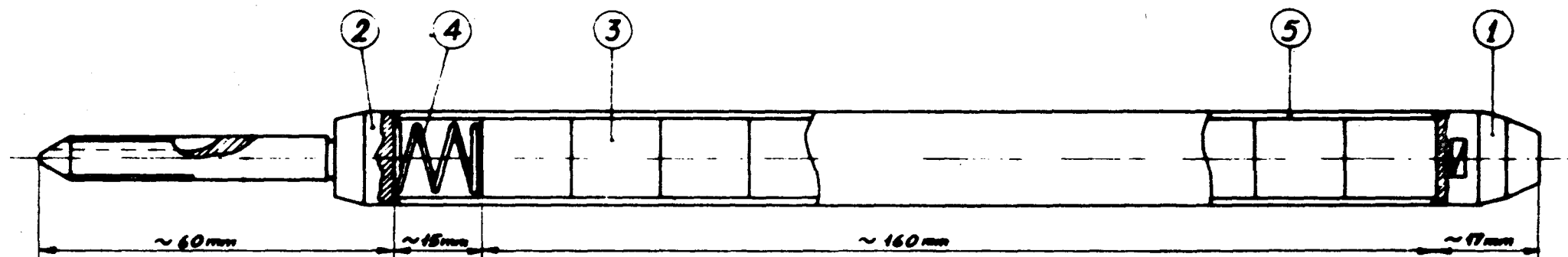
2.2 Measurements

The measurement program was subdivided into the three following stages:

- a) Measurement of the neutron flux in the irradiation channel
- b) Development of the measurement system and pin irradiation
- c) Miscellaneous measurements.

The thermal neutron flux measurements in the position where the short pins were to be located were taken between May 6 and 12, 1968. Copper disc monitors, 9 mm in diameter and 0.2 mm thick, were irradiated in pairs, one disc being cadmium-coated to provide the epithermal component. After irradiation, a 2"x2" photoscintillator and a multi-channel analyzer were used for the counting.

The neutron flux distribution along the channel was first measured with a tungsten wire and then with a copper wire. The channel in question is normally used for inserting neutron counters as part of the reactor control equipment; it crosses the main biological shield obliquely till it emerges in the gap between the shield and the pressure vessel in correspondence of the core, and then returns inside the shield wall. Part of the channel length facing the core is surrounded by a lead sleeve.



ITEM	DESCRIPTION	N. off	MATERIAL
1	END CAP	1	ZIRC 2
2	THREADED END CAP	1	ZIRC 2
3	FUEL PELLET	11	PuO_2/UO_2
4	RETAINING SPRING	1	E.N. 49
5	CAN	1	ZIRC. 2

FIG. 3-11 - PLUTONIUM OR ENRICHED URANIUM SHORT PINS USED IN PRELIMINARY MEASUREMENTS

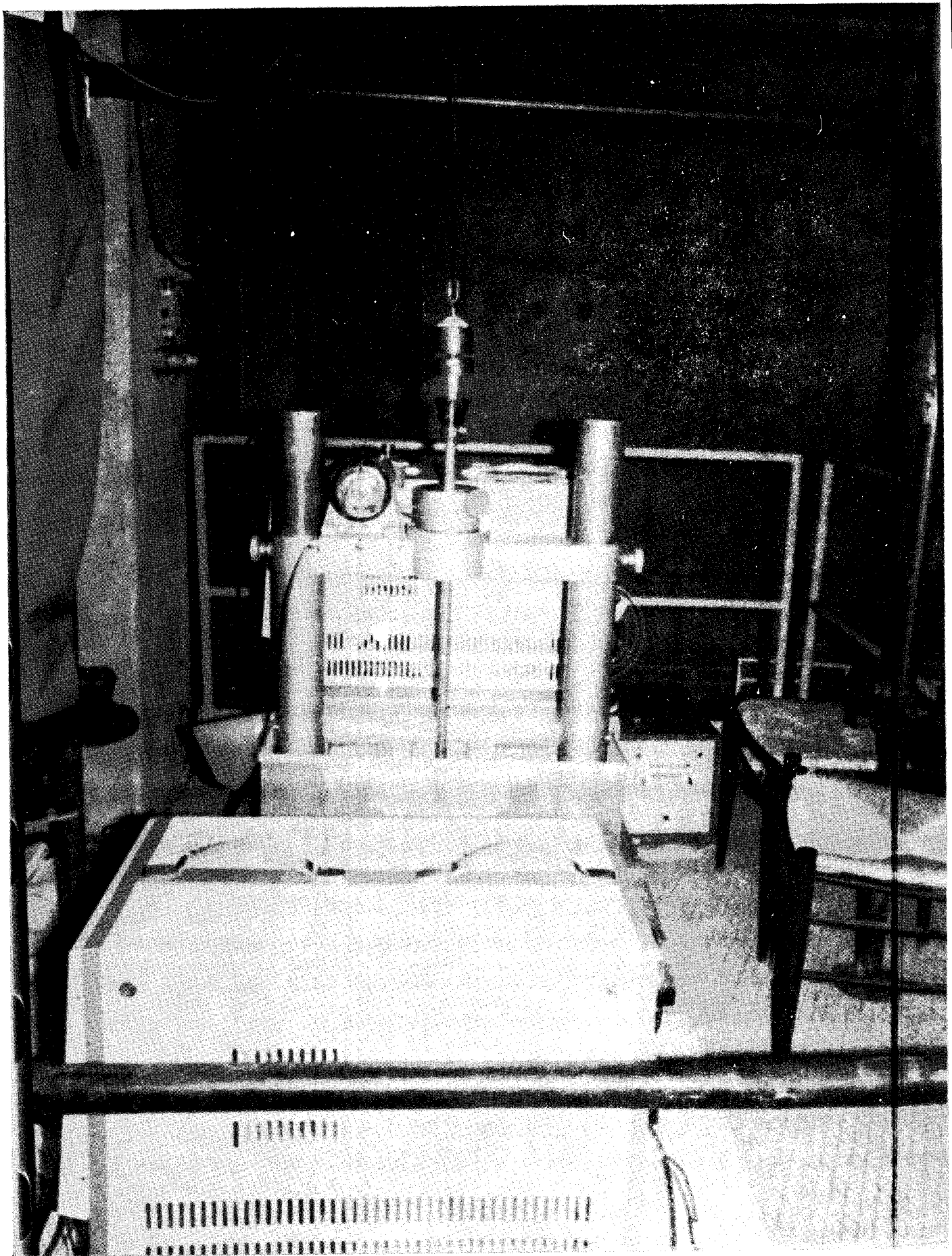


FIG. 3-12 - FUEL ROD POSITIONING MECHANISM FOR
GAMMA-SCANNING

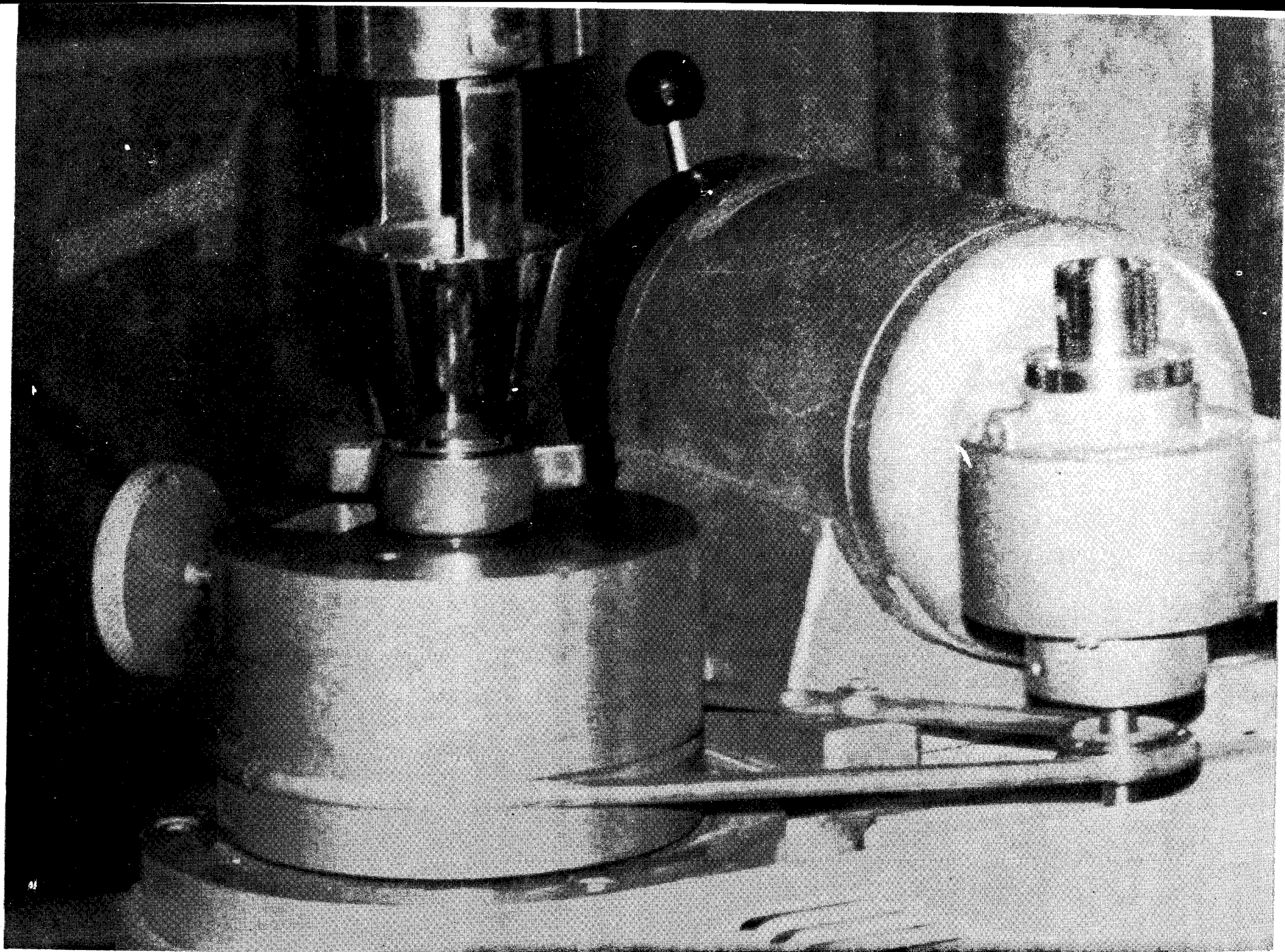


FIG. 3-13 - FUEL ROD ROTATING MECHANISM FOR GAMMA-SCANNING

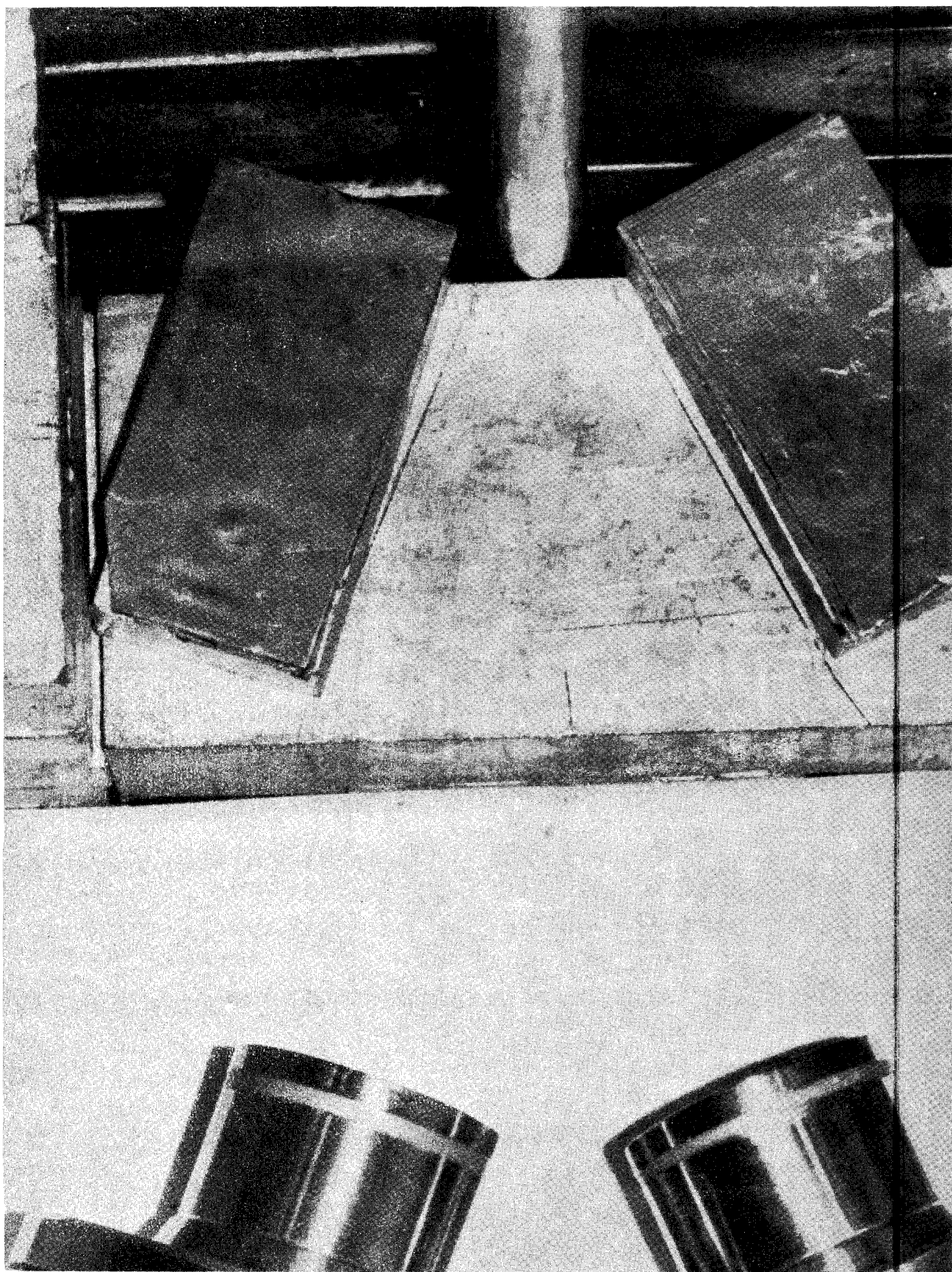


FIG. 3-14 - SHIELD AND COLLIMATION SYSTEM

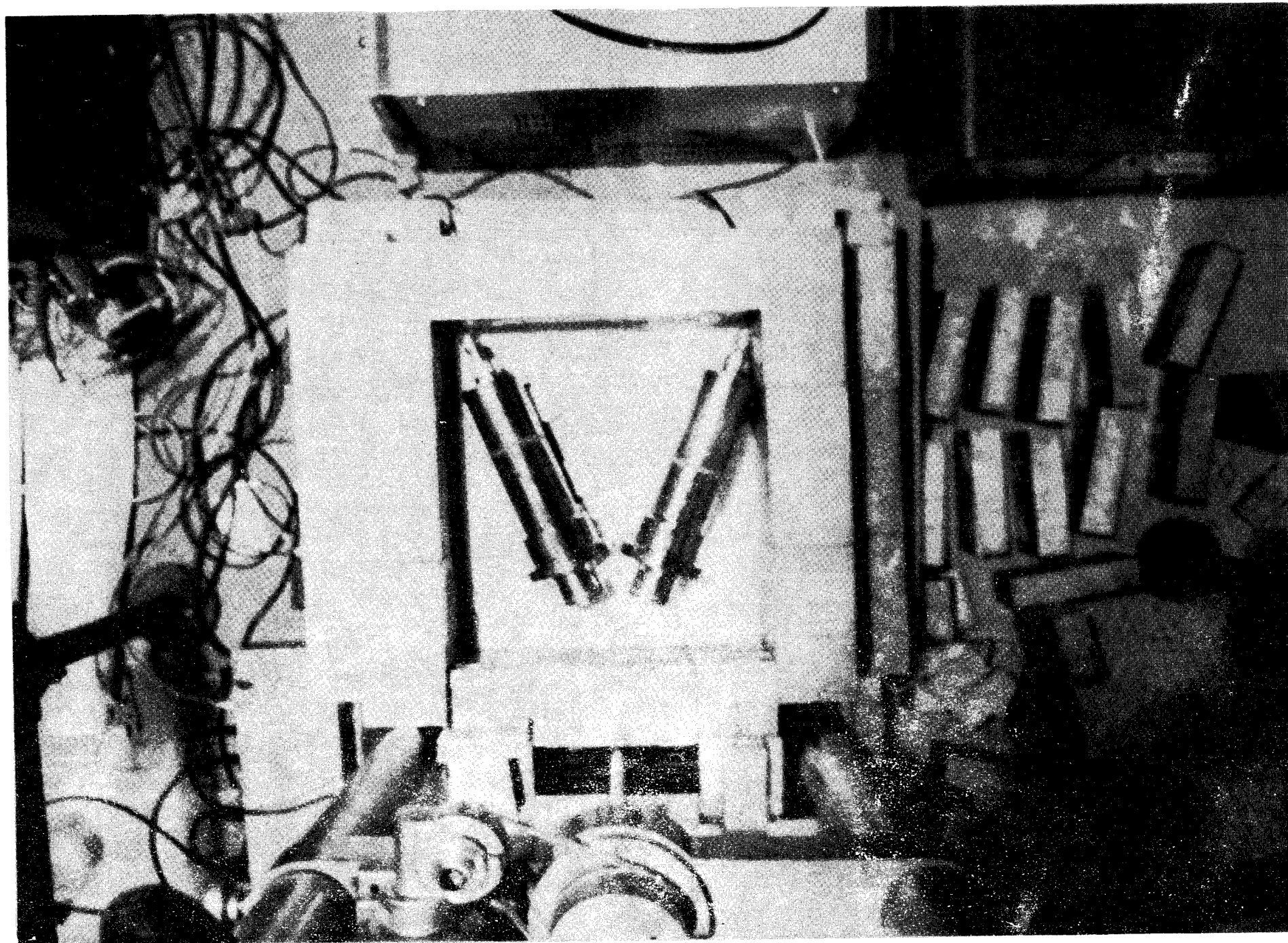


FIG. 3-15 - VIEW OF GAMMA-SCANNING MEASUREMENT SYSTEM

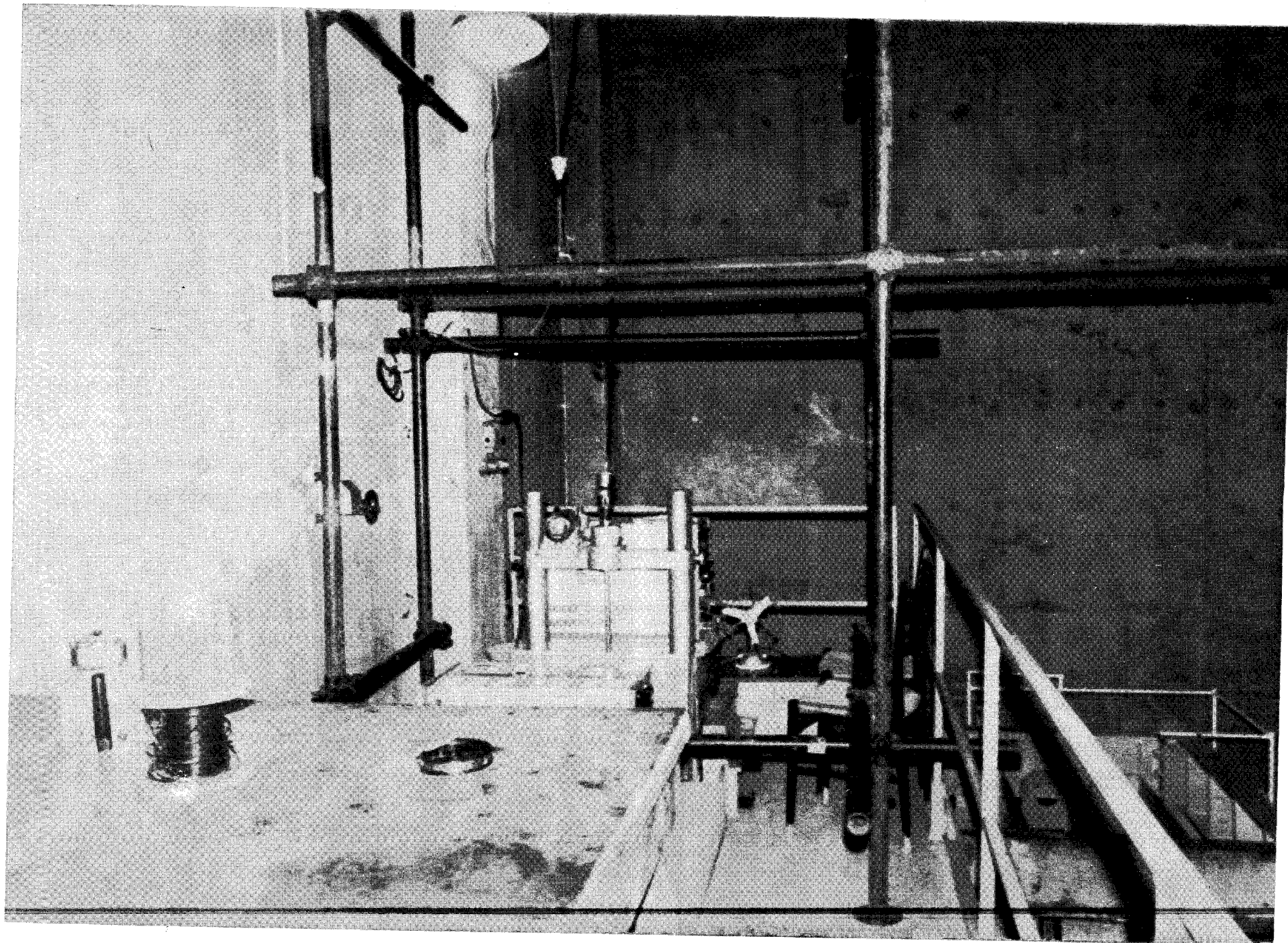


FIG. 3-16 - SCAFFOLDING FOR GAMMA-SCANNING EQUIPMENTS

Fig.3.17 shows the thermal neutron flux distribution in this channel. It will be noted that the only area with an acceptable flux gradient lies between 11.5 and 12.5 meters' depth. This was the area selected for pin irradiation.

During the second stage, completed on May 19, the shield was built, the detector chains were calibrated and the first adjustments in the measurement technique were made.

Three pins, one of each type, were irradiated one hour each together with the flux monitors. The thermal neutron fluxes and the cadmium ratio for the three pins were:

	ϕ , n/cm ² /sec	CR
U pin	$5.0 \cdot 10^9$	6.4
Pu - Type A pin	$3.1 \cdot 10^9$	4.4
Pu - Type C pin	$2.7 \cdot 10^9$	3.6

The day after the irradiation, the fission product distribution along the three pins was measured. The results of this measurement is given in Fig.3.18, and it indicates that the distribution is rather uniform in the central part of the three pins.

The short pins were then inserted in one of the guide tubes for the other measurements.

The third stage began on May 19 and was completed on June 19. It covered the main measurements, namely,

- Measurement of the background radiation spectra and specimen spectra at different times.
- Measurement of the radiation level on the guide tube surface in correspondence of the specimens.

Measurement (a) was taken twice a day during working days and once a day on holidays. Measurement (b) was always taken once a day.

2.3 Gamma measurements

After a few modifications, the technique for the measurement of gamma ray spectra was finalized on May 23, as follows:

- The guide tubes carrying the pins were placed on the gamma scanning equipment at a certain constant angle.
- The analyzer was calibrated on 400 channels, with a threshold at 200 keV, corresponding to 5 keV/channel.
- A reference peak of 480 keV as used for the gross gamma scan and integration was extended from the tenth channel before this peak to all the remainder of the spectrum.

Date: 7-5-68
Thermal power: 480, 8 MW

Electrical power: 154 MW
Max Flux peak : 3×10^9 n/cm² sec.

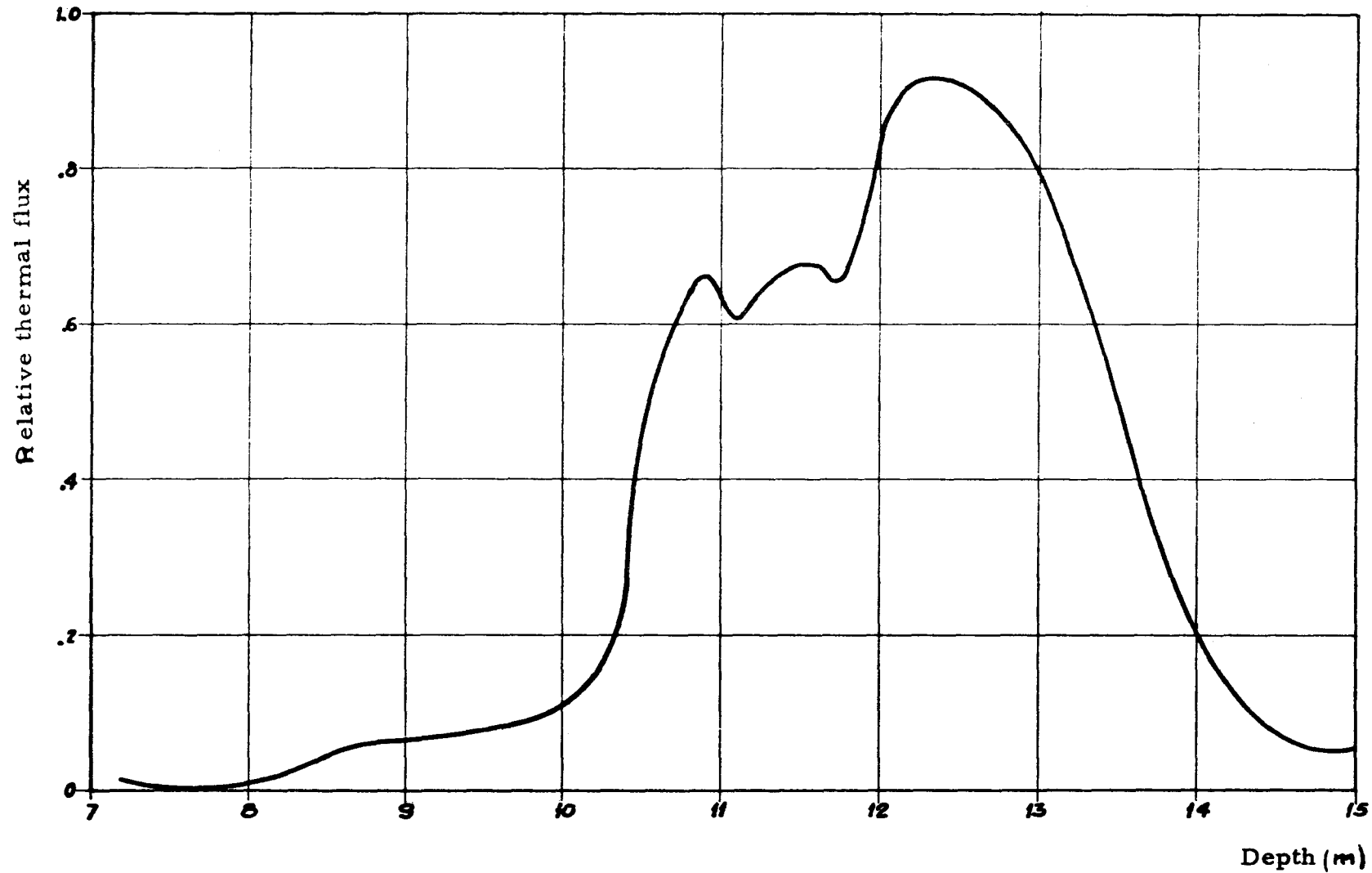


FIG. 3-17 - THERMAL NEUTRON FLUX DISTRIBUTION ALONG THE
CHANNEL CHOSEN FOR SHORT-PIN IRRADIATION

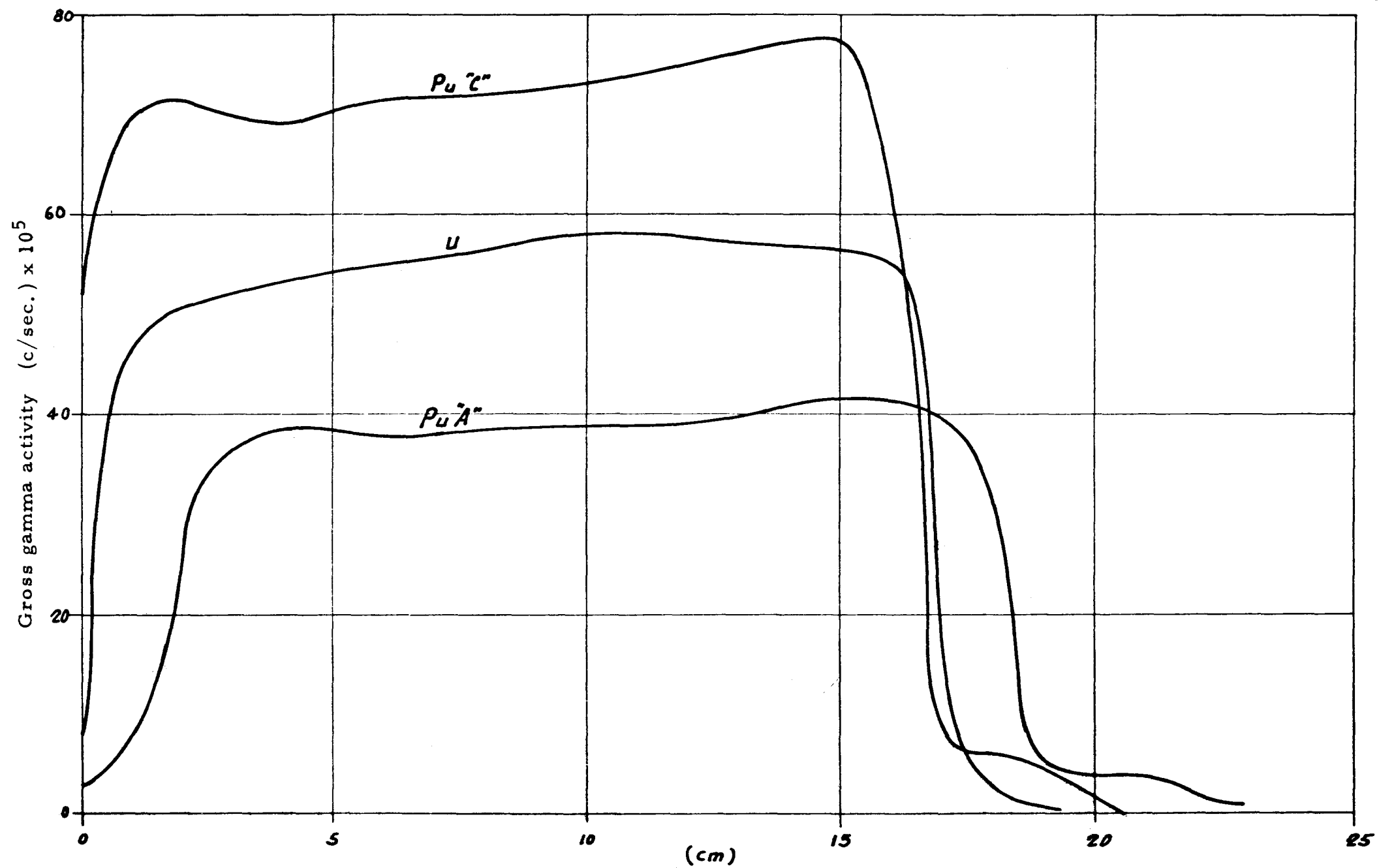


FIG. 3-18 - GAMMA-ACTIVITY ALONG THE THREE SHORT PINS

- d) Since the 480-keV reference peak did not always occur in correspondence of the same channel, a correction was made for the asymmetry of the peak channel by means of a computer program which determines a fraction of a channel used as the starting point.
- e) The 1.6 MeV La-140 peak occurred between channels 268 and 272; by adjusting the amplification it was possible to keep the peak within these limits except for a short period. However, it was experimentally proved that even when the peak shifted to channel 277, the integral remained constant within the measurement error. The integration was performed on 40 channels, the first and last being selected across the peak so that the line joining them was horizontal. When this was not possible, two adjacent integrals were averaged so that the lines joining the channels at the extremes intersected.
- f) The background radiation was measured a first time with the unirradiated pins in front of the collimator and immediately after without the pins. Subsequently, the background radiation was measured every day without the pins. The difference between the first two measurements represented the radiation contributed by the unirradiated uranium and plutonium, for which all the spectra were to be corrected. Instead, the daily measurements gave the external radiation which must be detracted from every spectrum.

2.4 Difficulties encountered during the measurements

- a) The high temperature in the measurement room, normally between 39 and 40°C, interfered considerably with the whole test. It particularly affected the operation of one of the two analyzers so that the second chain was in service only for a limited number of days. Moreover, it was not deemed advisable to keep the instrument in continuous operation, and the scheduled automatic night measurements were given up.
- b) The rotating equipment could not be used at that time as it had not been completed.
- c) Sometimes the spectrum integrator gave erroneous results, so that all integrations had to be performed by hand. This inconvenience, however, appeared to be due to the high temperature, because when the instrument was brought to a room temperature of about 20°C it operated continuously for 24 hours and always gave correct results.
- d) The background radiation increased considerably when six plutonium-enriched fuel elements were brought into the measurement room. The variation was threefold in the gross gamma integration range, and twentyfold in the lanthanum peak integration range. At any rate, the actual background value, measured daily, was always taken into account.

2.5 Test results

2.5.1 Radiation levels

Table II gives the radiation levels measured on the surface of the guide tube in correspondence of the three pins. The values were obtained with two different portable ion chambers: CUTIE PIE (CP) and ECKO 555. The discrepancies between the two sets of values depend on the larger sensitive area of ECKO which tends to average the levels and thus does not permit a good localization of the point of measurement. Fig.3.19 gives the radiation versus time curve, normalized for a thermal neutron flux of 1×10^9 n/cm²/sec for the pin with the highest activity, that is, the type C plutonium pin with 2.855% of fissile plutonium.

2.5.2 Gamma spectrometry

Table III summarizes the results of the gamma spectrometry observations for the period between 15 and 30 days after irradiation. Column 1 gives the number of filed spectra. Column 2, subdivided in three parts, gives the date, the time of the measurement, and the interval between irradiation and measurement. Column 3, also subdivided in three parts, one for each pin, gives the gross gamma integral expressed in pulses per second, net of the background and pin activity. Column 5 gives the time function, $f(t)$, for La-140 decay.

2.6 Analysis of the results

2.6.1 Gross gamma measurements

On the basis of the technical literature, an analytical expression was sought to express the results (C) of the gross gamma scanning in the form:

$$C = A t^{-B}$$

where A is constant for a given neutron flux, macroscopic fission cross-section, detection efficiency and geometry of the source;

B is constant for each type of fuel.

The following expressions were found for the three pins:

U pin	$C = 890,000 t^{-1.401}$
Type A Pu pin	$C = 654,460 t^{-1.1610}$
Type C Pu pin	$C = 1,532,000 t^{-1.1876}$

The cooling time during which these expressions are applicable is the period between the 15th and 30th day after irradiation, but the expressions can certainly be extrapolated for a few days beyond this interval.

The deviations between the theoretical values obtained with this formula and the experimental values are given in Table IV as a function of cooling time. It will be noted that notwithstanding the balance between

TABLE II

RADIATION LEVELS (mR/h)

DATE		CUTIE PIE			EKCO 555		
Days	ΔT^* Days	U	Pu "A"	Pu "C"	U	Pu "A"	Pu "C"
13 -5	0	-	-	250,000	-	-	-
14 -5	0,7	-	-	500	-	-	-
16 -5	1,6	-	-	100	-	-	-
17 -5	2,7	-	-	70	-	-	-
20 -5	5,6	-	-	44	-	-	-
21 -5	6,6	-	-	34	-	-	-
22 -5	7,6	24	20	31	25	21	31
23 -5	8,7	21	17	25	20	18	28
24 -5	9,6	18	15	24	18	15	20
25 -5	10,7	17	13	22	17	15	25
26 -5	11,7	13	11	21	14	13	20
27 -5	12,6	14	13	20	14	12	14
28 -5	13,6	-	-	-	12	11	18
29 -5	14,6	-	-	-	13	11	18
30 -5	15,6	11	9	14	11	11	15
31 -5	16,6	7	5,5	11	13	10	17
1 -6	17,7	7	6	10,5	10	8,5	14
2 -6	18,7	7	6	11	8,5	8,5	11
3 -6	19,6	6	5,5	8.5	-	-	-
4 -6	20,6	5,5	5	8.5	-	-	-
5 -6	22,0	5	5	8.5	8	7	11
6 -6	22,7	5	5	7	7	7	13
7 -6	23,6	5	4,5	7	7	5,5	9
8 -6	24,7	5	4,5	7	7	6	10
9 -6	25,7	5	4	5.5	6	5,5	9
10 -6	26,6	4,5	4,5	7	5,5	5,5	10
11 -6	27,6	5	5	7	5,5	5,5	8
12 -6	28,6	5	4	6	5	5	8

* Time 0: end of irradiation

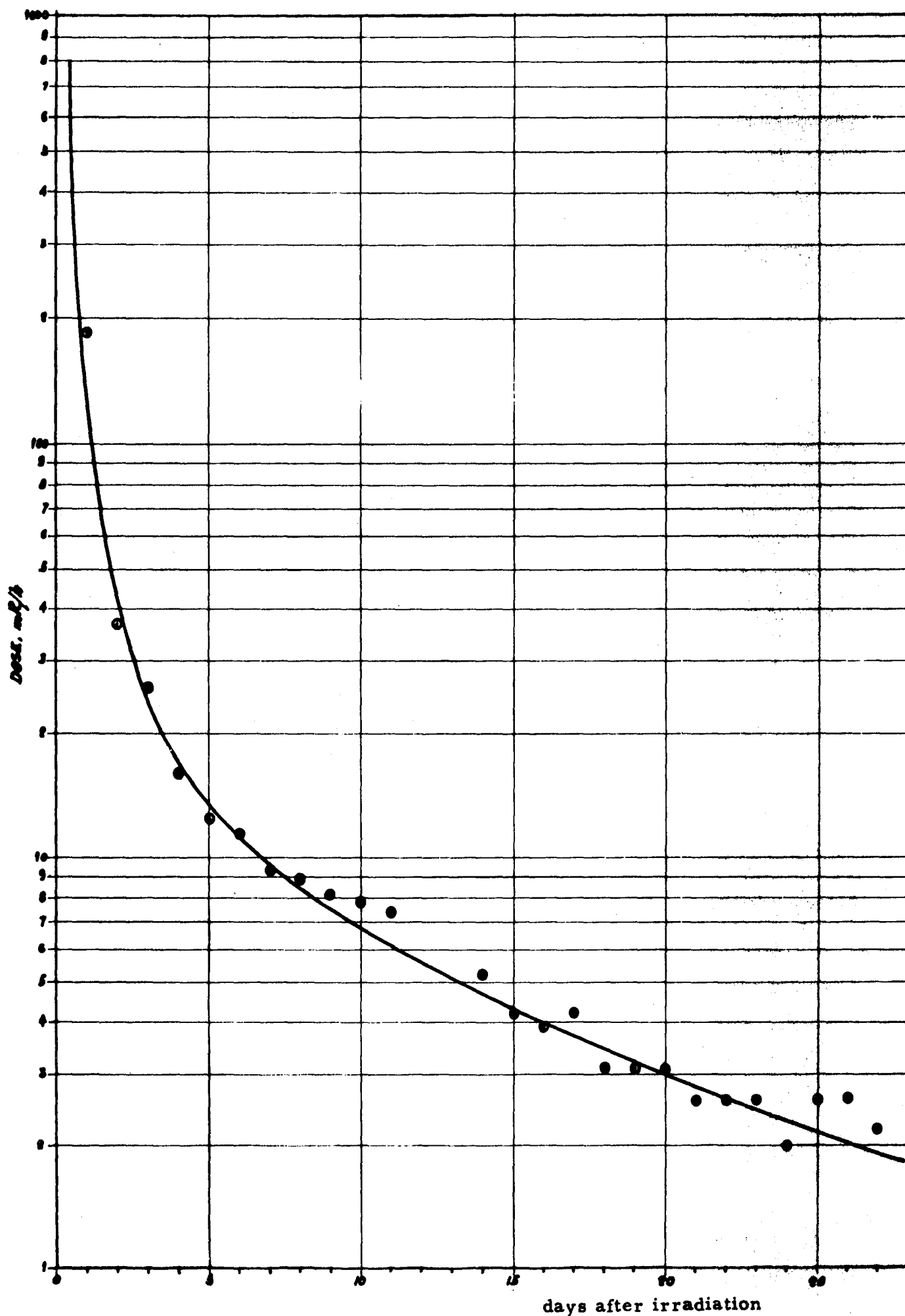


FIG. 3-19 - DOSE VARIATION VERSUS TIME FOR THE Pu "C" PIN
(Pu f 2.855%) NORMALIZED FOR A THERMAL NEUTRON
FLUX OF 10^9 n/cm² s

TABLE III

ANALYSIS OF SPECTRA - CHAIN I

(Values of integrals in cps)

N. Spectrum	DATE			GROSS-GAMMA INTEGR.			La ¹⁴⁰ INTEGR.			f(r)
	Day	Hour	Δ T, h	U	Pu "A"	Pu "C"	U	Pu "A"	Pu "C"	
16	27-5	16, 30	335, 0	1170, 5	770, 5	1547, 3	95, 7	57, 4	113, 1	0,4667
17	28	9, 30	352, 0	1110, 6	715, 7	1447, 8	93, 0	55, 0	108, 0	0,4498
18	28	16, 00	358, 5	1091, 7	703, 7	1413, 7	90, 7	54, 4	107, 0	0,4434
19	29	10, 30	377, 0	1022, 7	667, 2	1332, 4	86, 8	52, 3	100, 4	0,4258
20	29	16, 00	382, 5	1010, 2	656, 0	1310, 6	85, 75	51, 4	100, 6	0,4207
21	30	10, 30	401, 0	953, 1	620, 5	1232, 9	82, 0	49, 0	96, 1	0,4037
22	30	17, 00	407, 5	949, 2	614, 4	1214, 5	81, 8	49, 1	95, 0	0,3980
23	31	10, 00	424, 5	898, 1	584, 1	1157, 8	77, 7	47, 4	91, 5	0,3833
24	31	16, 00	430, 5	884, 9	574, 5	1138, 6	76, 7	46, 0	90, 2	0,3781
25	1-6	11, 30	450, 0	836, 2	548, 7	1046, 6	73, 1	44, 5	85, 7	0,3620
26	2	11, 00	473, 5	796, 3	506, 4	1018, 1	70, 05	41, 2	80, 5	0,3434
27	3	10, 00	496, 5	758, 7	484, 5	964, 4	66, 2	39, 96	77, 2	0,32616
28	3	16, 30	503, 0	748, 9	478, 8	948, 5	65, 8	39, 0	76, 4	0,3214
29	4	10, 00	520, 5	714, 5	462, 4	910, 1	62, 3	38, 4	73, 0	0,3093
30	4	16, 00	526, 5	703, 1	455, 7	896, 2	60, 8	37, 0	72, 2	0,30475
31	5	17, 30	552, 0	672, 2	429, 6	852, 8	58, 9	35, 3	68, 1	0,2878
32	6	11, 00	569, 5	649, 7	412, 8	821, 0	56, 8	33, 7	65, 5	0,2733
33	6	16, 30	575, 0	643, 7	406, 3	810, 3	56, 3	33, 3	64, 7	0,2733
34	7	10, 00	592, 5	613, 8	399, 4	783, 3	53, 5	32, 2	62, 8	0,2627
35	7	16, 30	599, 0	610, 2	394, 6	774, 2	52, 8	31, 5	62, 2	0,2589
36	8	11, 00	617, 5	591, 2	377, 8	746, 4	50, 45	30, 1	58, 8	0,2484
37	9	10, 30	641, 0	568, 1	357, 0	712, 9	48, 1	28, 3	56, 0	0,2355
38	10	10, 00	664, 5	535, 2	347, 0	682, 3	45, 0	26, 9	53, 3	0,2234
39	10	16, 30	671, 0	528, 5	345, 7	675, 6	44, 1	26, 95	52, 6	0,2201
40	11	9, 30	688, 0	516, 5	332, 8	654, 3	43, 0	25, 95	50, 1	0,2119
41	11	16, 30	695, 0	509, 1	327, 6	645, 5	42, 3	25, 6	49, 9	0,20855
42	12	10, 00	712, 5	497, 2	319, 6	623, 0	41, 4	24, 6	47, 60	0,20044
43	12	16, 00	718, 5	493, 3	315, 2	622, 8	40, 24	24, 18	47, 23	0,19775
44	13	11, 30	739, 0	475, 0	304, 6	599, 0	38, 8	22, 9	44, 8	0,18885
45	14	11, 00	762, 5	453, 9	291, 9	578, 6	36, 27	21, 87	42, 74	0,17908

TABLE IV

PERCENTAGE DEVIATIONS BETWEEN CALCULATED AND EXPERIMENTAL VALUES

N. Spectrum	$\Delta T, h$	GROSS GAMMA			¹⁴⁰ La		
		U	Pu "A"	Pu "C"	U	Pu "A"	Pu "C"
16	335,0	0,57	- 0,53	-0,60	-0,59	-0,52	-1,73
17	352,0	0,17	1,09	0,10	- 1,43	0,06	-0,79
18	358,5	0,19	0,65	0,30	-0,35	-0,27	-1,30
19	377,0	0,59	0,15	0,20	-	-0,38	0,02
20	382,5	9,20	0,15	0,10	-	0,14	-0,38
21	401,0	0,60	0,24	0,70	0,35	0,79	0,06
22	407,5	-0,82	-0,66	0,20	-0,82	-0,83	-0,20
23	424,5	0,06	-0,33	0,20	0,55	-1,07	-0,21
24	430,5	-0,06	-0,30	0,20	0,48	0,56	-0,15
25	450,0	0,55	-0,86	-	0,93	-0,47	0,61
26	473,5	-0,37	1,25	0,10	-0,07	1,94	1,58
27	496,5	-0,94	0,19	0,10	0,42	0,13	0,63
28	503,0	-1,12	-0,15	-	-0,43	0,82	0,20
29	520,5	-0,31	-0,72	-	1,18	-1,47	0,91
30	526,5	-0,01	-0,51	0,20	2,12	0,76	0,54
31	552,0	-0,92	-0,09	-0,30	-0,40	-0,24	0,66
32	569,5	-1,07	0,27	-0,20	-0,70	0,45	0,62
33	575,0	-1,24	0,73	-0,10	-1,06	0,41	0,61
34	592,5	0,10	-1,04	-0,30	0,08	-0,18	- 0,35
35	599,0	-0,56	-1,10	-0,40	-0,05	0,55	- 0,85
36	617,5	-0,85	-0,27	-0,30	0,36	0,96	0,62
37	641,0	-1,14	1,05	-0,20	-0,20	1,78	0,17
38	664,5	0,72	-0,29	-0,10	1,17	1,58	-0,16
39	671,0	1,53	-0,35	0,40	1,70	-0,07	-0,32
40	688,0	0,33	-0,15	-	0,44	-0,09	0,74
41	695,0	0,61	0,27	-	0,49	-0,32	-0,44
42	712,5	0,14	-0,16	0,60	-0,59	-0,30	0,30
43	718,5	-0,02	0,25	-0,20	0,17	0,06	-0,26
44	739,0	0,54	0,42	0,20	-0,79	0,89	-0,41
45	762,5	1,52	1,02	-	0,63	0,18	-0,19
negative deviations		14 (-)	16 (-)	11 (-)	13 (-)	14 (-)	14 (-)
zero deviations				5 (o)	2 (o)		
positive deviations		16 (+)	14 (+)	13 (+)	15 (+)	16 (+)	16 (+)

negative and positive deviations, the distribution of the points suggests a discrepancy between the analytical expression and the experimental results.

At any rate, the formula was accepted because, within an error of 1%, it provides a linear interpolation for fuels whose enrichment is intermediate between the enrichments of the fuels used for the tests according to the following formula:

$$B = \frac{\sigma_f^5 \cdot \rho^5 \cdot \alpha + \sigma_f^9 \cdot \rho^9 \cdot \beta}{\sigma_f^5 \cdot \rho^5 + \sigma_f^9 \cdot \rho^9}$$

where $\sigma_f^{5,9}$ are the fission cross-sections for U-235 and Pu-239
 $\rho^{5,9}$ are the enrichments in U-235 and Pu-239, respectively
 α, β are the indexes for U-235 and Pu-239, respectively.

Since for enriched uranium $\alpha = 1.1401$, and assuming $\sigma_f^9 / \sigma_f^5 = 1.38$ which corresponds to a Maxwell spectrum, the formula applied to type C fuel gives $\beta = 1.198$. With these values of α and β it is possible to compile decay tables for the various types of fuel that will be used during the measurements in order to refer the experimental data to a given time.

2.6.2 La-140 measurement

The data in Table III, referred to the period between the 15th and 30th day of cooling, were used to determine the apparent halftime for the three fuels according to the minimum square method. The following values were obtained:

U	h. t. = 12.79 days $\pm 1\%$
Type A Pu	h. t. = 12.78 days $\pm 1\%$
Type C Pu	h. t. = 12.79 days $\pm 1\%$

As one can see, the deviation from the value of 12.8 days given in the literature is within the experimental error.

The deviations between theoretical and experimental values are listed in Table IV as a function of cooling time. The standard deviation with a 95% confidence level is comprised between the following limits:

0.64 - 1.08 for U
0.63 - 1.06 for Type A Pu
0.55 - 0.92 for Type C Pu

As a result, within the time interval considered, the 1.6-MeV lanthanum peak can be reduced to a common time for the three types of fuel by means of the theoretical function $f(t)$.

2.6.3 Relationship between the two counting chains

So far, only the data of chain 1 have been analyzed. In fact, chain 1 operated continuously, whereas chain 2 permitted only a limited number of measurements and, owing to its low printing speed, it did not permit complete spectra to be preserved.

At any rate, by performing the same kind of calculations which led to the compilation of Table III, and by dividing the values in Table III by the corresponding ones of chain 2, the results tabulated in Table V were obtained. The ratio between values is always very near unity; this means that, within an error of 1-2%, the two chains are identical from the standpoints of efficiency and geometry.

2.6.4 Determination of the radiation levels

If on the basis of the data in Table II and Fig.3.19 we wish to determine the radiation level on the surface of the upper part of the fuel element to be disassembled and re-assembled for gamma scanning, it is necessary to start with a few empirical-theoretical considerations. Owing to the complex geometry and difficult location of the points of measurement, it is necessary to keep to a mere estimate of the order of magnitude of the radiation levels. In doing this, the following data must be taken into account:

- a) Unirradiated pins have a surface radiation level of about 1 mrem/h.
- b) Irradiated pins, after 15 days' decay, have a surface radiation level of about 10 mrem/h.
- c) Unirradiated fuel elements stored in the measurement room have a surface radiation level of 5 mrem/h at mid height and 0.5 mrem/h at the top.
- d) Since the neutron flux for these measurements will be twice the flux for the preliminary measurements, through a simple proportion we may expect to have a surface radiation of 100 mrem/h at mid height of the irradiated element and 10 mrem/h at the top after 15 days' decay.
- e) The adoption of a safety factor of 3 is also recommended in order to take into account any inaccuracies in the measurements, the approximate assumptions at the basis of the calculation, and the possibility that the neutron flux is higher than anticipated.

In view of the foregoing, the following average surface radiation levels are to be expected:

- less than 30 mrem/h at the top of the element
- less than 300 mrem/h at mid height of the element.

TABLE V

RATIOS BETWEEN THE DATA OF THE TWO COUNTING CHAINS

N. Spectrum	$\Delta T, h$	GROSS GAMMA			LANTANIO		
		U 2,4%	Pu "A"	Pu "C"	U 2,4%	Pu "A"	Pu "C"
32	569,5	0,9949	-	0,9999	1,0125	0,8553	1,0077
33	575,0	1,0072	1,0125	-	1,0199	1,0215	0,9985
34	592,5	1,0026	1,0104	1,0169	1,0113	1,0158	1,0145
35	599,0	1,0126	1,0082	1,0150	1,0000	1,0194	1,0130
36	617,5	1,0137	1,0093	1,0124	0,9980	1,0033	0,9932
37	641,0	1,0149	0,9969	0,9971	1,0148	1,0000	0,9947
38	664,5	0,9940	0,9847	0,9972	1,0022	0,9890	1,0038
39	671,0	1,0051	1,0169	1,0152	0,9977	1,0187	1,0333
40	688,0	0,9943	1,0099	1,0009	0,9953	1,0097	0,9891
41	695,0	1,0033	1,0021	1,0148	0,9952	1,0322	1,0309
42	712,5	1,0080	1,0050	0,9996	1,0081	1,0081	1,0042

2.7 Conclusions

- a) The instrumentation provided for the measurements proved to be adequate as long as the room temperature remained within acceptable limits (20-25°C).
- b) It is advisable to increase the shield thickness to allow for the larger number of fuel elements present during the measurement.
- c) The element should be irradiated for one hour and, to improve counting statistics, the maximum neutron flux on the 3x3 assembly should be 5×10^9 n/cm²/sec at the elevation of the point of measurement.
- d) Measurements should preferably not start before 15 days' cooling.
- e) The procedure described in paragraph 2.8 below takes about an hour in total for the measurements on one rod, exclusive of rod handling and repetitions in the event of erroneous measurements and instrument malfunctioning. The procedure tends to exclude instrumentation and integration errors; statistical errors can be taken to be on the same order as those of the preliminary measurements, i.e. 1% with a confidence level of 95%.

2.8 Proposed procedure for the measurements during the refueling outage

- a) Use will be made of the same instrumentation utilized for the preliminary measurements, namely, two phototubes, two analyzers, and the lead shield with a 3-cm slot. The only difference will be the raising of the shield base by 40 cm to permit axial scanning of the whole rod (active length 275 cm).
- b) The analyzers will be calibrated in the same way as for the preoperational tests, that is, with a threshold at 200 keV, and analysis of 400 channels up to 2.2 MeV.
- c) Integration for gross gamma radiation will start 10 channels before the 480-keV peak and continue for 100 channels after the beginning of the lanthanum peak. The integration for lanthanum will be extended to 40 channels according to the technique described earlier.
- d) The complete measurement of a rod will consist of the following operations:
 - (1) 10-minute counting
 - (2) Print-out of the spectrum of chain 1
 - (3) Integration for lanthanum and gross gamma scan on the two chains with double print-out of the integral
 - (4) New print-out of the spectrum of chain 1 to check that the memory content has not changed
 - (5) Repetition of operations 1 to 4 twice
 - (6) At this point, all integrals will be referred to a common time with the aid of the tables giving the time functions for lanthanum and gross gamma radiation. The resulting values from the two measure-

ment chains must be consistent; in the negative, it is necessary to find out which chain gave erroneous results and possibly also repeat the measurement from the beginning.

- e) After every two or three rods, it is necessary to measure the background activity and to check the instrumentation efficiency by means of a calibrated source, according to the procedure in d) above.
- f) Three short pins of the type used for the preliminary measurements will be irradiated in a dummy element next to the 3x3 critical assembly and then subjected to counting as described in d).
- g) For each rod, the axial distribution of the fission products will be determined by means of the analyzer of chain 1 in multiscaler position and by integrating over the whole spectrum between 200 keV and 2.2 MeV. Tentatively, the sequence should include one measurement every 10 cm for 20 seconds at 5-second intervals during which the rod will be moved manually to the next position.

TASK IV - ISOTOPIC COMPOSITION MEASUREMENTS ON IRRADIATED URANIUM FUEL

To integrate the experimental results available for the development of the calculation method under Task II, isotopic composition measurements and gamma scanning will be performed on a few uranium rods of one of the fuel elements discharged during the May 1967 shutdown, namely element A-106.

The measurements will be performed by the Institute for Transuranic Elements of the Common Research Center at Karlsruhe in the second half of 1968.

The work performed in connection with this task includes the preparation of a schedule for non-destructive (gamma scanning) and destructive (isotopic composition) tests, and the study of the problems associated with the transport of the irradiated fuel rods from the Garigliano station to the Karlsruhe Center.

1. Schedule of tests to be performed on rods of element A-106

The element selected for the tests is A-106 which had reached an average burnup of about 9500 MWD/t when it was discharged on May 27, 1967. The average isotopic composition estimated from calculations performed on a tentative basis by ENEL is as follows:

U-235	1.18%
Total Pu	0.44%
Pu-239	0.32%
Pu-240	0.08%
Pu-241	0.03%
Pu-242	abt 0.005%

This element was selected because for the following reasons it lends itself well to provide a confirmation of the validity of the calculation methods used in the design:

- a) it has reached a sufficiently high burnup level so that the plutonium content is of the same order as the U-235 content;
- b) it was located in a sufficiently central core location to minimize the effect of power tilting;
- c) it was not affected by the proximity of control rods during the last 2000 MWD/t or so of burnup.

The knowledge of the power distribution during the last days of residence in the reactor would be very useful for the purpose of an

integral verification of the burn-up calculation code. However, owing to the long time this element has had to decay, it is felt that the above-mentioned tests would no longer be meaningful. Thus, gamma scanning will be performed only to determine the burn-up distribution. At any rate, the fission product nuclides to be monitored for the gamma scan will be selected when the rods are delivered at Karlsruhe and the intensity of the signal has been verified. Actually, provisions have been made for a complete spectrum analysis to be performed with a 4000-channel analyzer to select the isotopes to be measured. Up to four scans can be performed simultaneously; two could be related to Cs-137 and Ce-144, while the other two will be established on the basis of the spectrum revealed during the measurements. Cs-137 generally presents diffusion phenomena, however, and Ce-144, which has a mean halftime of about 280 days, will provide information only on the last year of residence in the reactor.

Since it is not yet possible to make an accurate assessment of the validity of the gamma scans, it has been decided to perform these measurements on a limited number of rods and to extend them to the others only if the results appear to be reliable.

The destructive test will consist of the chemical analysis of the isotopic content. Rod lengths of about 10-15 mm will be isolated, from which to take the test specimens. Each set of tests will include the following determinations:

- a) Burn-up level, through the measurement of the long-lived fission nuclide content. The Nd-148/U measurement technique will be adopted because the Cs-137 technique more commonly used in the past may give unreliable results as a result of cesium diffusion.
- b) Pu/U, Am/U and Xe/U concentration ratios.
- c) Percentage contents of Pu-239, Pu-241, Pu-242, U-235, U-236, U-238 and of the isotopes of Am, Nd, Xe and Kr.

The desired number and precision of the analyses will be set later on when the results of the gamma scanning and other work are available. In fact, both the number and the precision will depend on the availability of laboratories, personnel and gamma scan results.

To integrate the information obtained from the two series of measurements, the internal pressure of the fission gases will also be determined before the rods are destroyed. The chemical analysis of the fission gases is rather complex; however, at least one gas sample will probably be analyzed.

Finally, the radial plutonium distribution in the rods will be measured as it may provide a useful indication of the fine structure of the flux inside a rod.

2. Problems associated with transport of irradiated fuel rods to the Karlsruhe Center

Element A-106 selected for the analysis described in the preceding paragraph had already been stripped in the reactor pool. The rods have been removed from the channel and are ready at the Garigliano for shipment to the Karlsruhe Center. For this purpose, two stainless steel baskets have been procured; the baskets are complete with spacer grids to accommodate the individual rods and permit their prompt identification.

For transport to Karlsruhe, various carriers were consulted and the only container capable of carrying the rods was found to be the 32-ton container owned by Transnucleaire, Paris. However, it has been ascertained that this container could not be handled by the facilities at the Karlsruhe Center. As a result, it was decided that the rods should be cut down in size to be shipped in a smaller container which could be handled at Karlsruhe. Since the Garigliano station is not equipped to perform the cutting, the following schedule was agreed upon:

- a) The rods of element A-106 will be transported in the 32-ton container from the Garigliano to the EUREX Center of CNEN in Saluggia, Vercelli.
- b) The rods will be cut in half.
- c) The cut rods will be transported from the EUREX Center to the Karlsruhe Center in 7.5-ton containers made available by Transnucleaire.

This schedule may be implemented commencing from the month of August 1968.

TASK VI - DETAILED STUDY OF PLUTONIUM FUEL CYCLES

1. Analysis for the positioning of plutonium elements in the Garigliano core at the beginning of cycle 2

At the end of Cycle 1C, eighty-three elements will be discharged from the Garigliano reactor and replaced with seventeen partially irradiated elements now in the fuel pool and sixty-six fresh fuel elements. Of the latter, 54 will be uranium elements with an average enrichment of 2.3%, and 12 will be plutonium elements (8 standard and 4 of the mixed type with UO_2 and $\text{PuO}_2\text{-UO}_2$ rods).

The purpose of this analysis is to determine the optimum positioning which will reconcile the requirement of a high burnup of the plutonium elements so as to collect in a sufficiently short time all the information expected from this power experiment, with the requirement of having power factors during the cycle which do not exceed those observed during the previous operation of the station.

In line of principle, the sixty-six fresh elements will be loaded according to a checkerboard pattern which excludes the peripheral zone of the core so as to provide the maximum insertion of reactivity. The positions of the plutonium elements were selected among these sixty-six to meet the requirements mentioned above.

The study of the fuel element positioning was based on the analysis of power density variations during Cycle 2. For this analysis use was made of the Haling technique which is incorporated in the FLARE code. This method permits the power distribution and core burn-up to be optimized over the entire cycle under consideration.

In practice, control rod withdrawal during operation is performed so that the actual power distribution will remain as near as possible the theoretical optimized distribution.

This analysis entails a general knowledge of the burn-up which the individual fuel elements of the first load will reach at the end of Cycle 1C. Again, this distribution was obtained by means of the Haling technique. At the same time, the nuclear constants to be introduced in the FLARE code were calculated for the three new types of fuel which will be loaded at the beginning of Cycle 2.

2. Characteristics of the reload fuel elements

The sixty-six fresh elements to be loaded into the Garigliano core at the end of Cycle 1C (August 1968) together with seventeen partially irradiated elements are broken down as follows:

- a) 54 UO_2 elements with an average enrichment of 2.3% in U-235
- b) 8 prototype $\text{UO}_2\text{-PuO}_2$ standard elements
- c) 4 prototype advanced elements containing UO_2 and $\text{UO}_2\text{-PuO}_2$ rods.

All these elements have bundles of 64 rods arranged in an 8x8 square lattice.

The main mechanical characteristics of the reload elements can be summarized as follows:

- a) All reload elements are interchangeable with those of the first core, both as concerns positioning on the support plate and control rod movement, and as concerns handling operating and facilities.
- b) The element is constituted of 64 rods (8x8) in a square array, clad in Zircaloy-2, with an outside diameter of 15.06 mm and an active length of 2718 mm.
- c) The supporting structure is constituted of two plates held together by eight peripheral fuel tie rods, two on each side of the element. The remaining rods rest on the lower plate and are free to expand through the upper plate, while being kept in position by a spring. Five equally spaced grids, plus the two end plates, ensure proper positioning of the rods. The spacer grids are of the type now adopted for BWR rods, that is, the rods are held steady by stainless steel wires on two sides of the cell and by Inconel springs on another side.
- d) One connector rod made up of six segments supports the five spacers of the element. The rod bundle is enclosed in a Zircaloy-2 sheath which is interchangeable with those of the first load.
- e) To allow for the swelling attendant on the higher burn-up, the clearance between the sheath and the fuel was increased to contain the stresses on the cladding.
- f) The fission gas plenum at the upper end of each rod was greatly increased with respect to the design of the first load because of the higher performance required of the fuel, both from the standpoint of the heat flux and of the burn-up level. A helical spring is inserted in the plenum to prevent pellet movement during transport and handling of the fuel elements.
- g) The fuel element has been designed for easy disassembly. For this purpose the end plugs of the various rods are different in size according to fuel type and enrichment so that proper repositioning of the rods is ensured.
- h) The upper plate and end piece, which were separated in the design of the first core element, are now cast in one piece; the same holds for the bottom end piece.
- i) Some of the pellets are dished to provide free space for their thermal expansion.

3. Reload uranium element

The rod enrichment values and distribution in the uranium fuel element are given in Fig. 6.1. The average enrichment is 2.3%. The ratio between the enrichment of the corner rods and that of the other rods is about the same as for the fuel of the first load.

4. Prototype standard plutonium elements

The rod enrichment distribution for this type of elements is given in Fig. 6.2. This element and the related nuclear design work were described in the report EUR 3890i, so that further details are not deemed necessary in this report.

5. Prototype advanced plutonium elements

The four prototype advanced elements are made up of forty enriched-uranium rods and twenty-four uranium-plutonium rods. The rod enrichment values and distribution are given in Fig. 6.3.

In order to avoid the formation of major power discontinuities inside an element between the enriched-uranium and the plutonium rods, the content of fissile plutonium in the plutonium rods adjacent to the uranium rods was lowered to 1.8% versus 2.89% of the inner rods.

The calculations performed for the advanced plutonium element revealed that it possesses the same reactivity lifetime as the reload enriched-uranium elements, but that in cold conditions the advanced element is more reactive than the "uncontrolled" enriched-uranium element by about $0.010 \Delta K$, and than the "controlled" uranium element by about $0.025 \Delta K$.

6. Preliminary determination of the core burn-up distribution at the end of Cycle 1C

The burn-up level reached by the individual elements at the end of Cycle 1B was calculated by means of the FLARE code. To simulate reactor operation, the following data were fed into the program every 200 MWD/MTU: actual control rod pattern, average thermal power values, core inlet subcooling and effective recirculation flow inside the fuel elements. Fig. 6.4 shows the distribution of average burn-up levels at the beginning of Cycle 1C after loading of fourteen fresh fuel elements.

The burn-up level that will be reached at the end of Cycle 1C was estimated on the basis of the power density distribution optimized with the Haling technique. The following assumptions were made as to the end-of-cycle conditions:

b	b	a	a	a	a	b	b
b	a	a	a	a	a	a	b
a	a	a	a	a	a	a	a
a	a	a	a	a	a	a	a
a	a	a	a	a	a	a	a
a	a	a	a	a	a	a	a
b	a	a	a	a	a	a	b
b	b	a	a	a	a	b	b

FIG. 6-1 - ROD ENRICHMENT DISTRIBUTION FOR RELOAD URANIUM ELEMENTS

a = 2.41 % U²³⁵ enriched rods

b = 1.83 % U²³⁵ enriched rods

U²³⁵ average enrichment: 2.3%

c	c	b	b	b	b	c	c
c	b	b	a	a	b	b	c
b	b	a	a	a	a	b	b
b	a	a	a	a	a	a	b
b	a	a	a	a	a	a	b
b	b	a	a	a	a	b	b
c	b	b	a	a	b	b	c
c	c	b	b	b	b	c	c

FIG. 6-2 - ROD ENRICHMENT DISTRIBUTION FOR THE PROTOTYPE STANDARD PLUTONIUM ELEMENTS

a = 2.85 w/o Pu^{fiss} containing rods

b = 1.40 w/o Pu^{fiss} containing rods

c = 0.74 w/o Pu^{fiss} containing rods

<i>d</i>	<i>d</i>	<i>c</i>	<i>c</i>	<i>c</i>	<i>c</i>	<i>d</i>	<i>d</i>
<i>d</i>	<i>c</i>	<i>c</i>	<i>b</i>	<i>b</i>	<i>c</i>	<i>c</i>	<i>d</i>
<i>c</i>	<i>c</i>	<i>b</i>	<i>a</i>	<i>a</i>	<i>b</i>	<i>c</i>	<i>c</i>
<i>c</i>	<i>b</i>	<i>a</i>	<i>a</i>	<i>a</i>	<i>a</i>	<i>b</i>	<i>c</i>
<i>c</i>	<i>b</i>	<i>a</i>	<i>a</i>	<i>a</i>	<i>a</i>	<i>b</i>	<i>c</i>
<i>c</i>	<i>c</i>	<i>b</i>	<i>a</i>	<i>a</i>	<i>b</i>	<i>c</i>	<i>c</i>
<i>d</i>	<i>c</i>	<i>c</i>	<i>b</i>	<i>b</i>	<i>c</i>	<i>c</i>	<i>d</i>
<i>d</i>	<i>d</i>	<i>c</i>	<i>c</i>	<i>c</i>	<i>c</i>	<i>d</i>	<i>d</i>

FIG. 6-3 - ROD ENRICHMENT DISTRIBUTION FOR PROTOTYPE
ADVANCED PLUTONIUM ELEMENTS

a = 2.89% Pu^{fiss} containing rods

b = 1.80% Pu^{fiss} containing rods

c = 2.41% U^{235} enriched rods

d = 1.83% U^{235} enriched rods

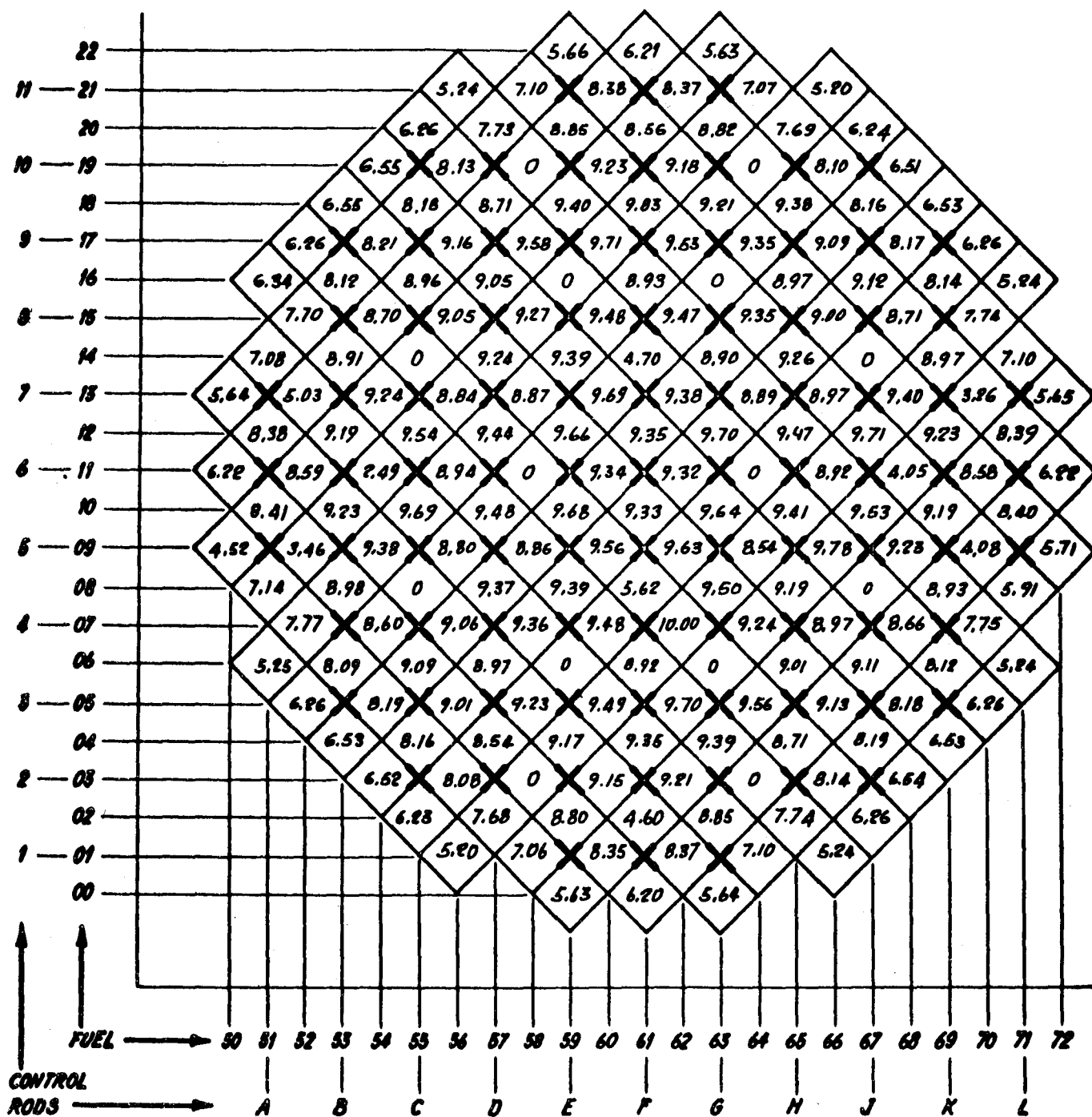


FIG. 6-4 - CICLE 1C:INITIAL DISTRIBUTION OF AVERAGE
BURN-UP LEVELS (10^3 MWD/MTU)

- a) all control rods out;
- b) sub-cooling: 36 Btu/lb;
- c) effective recirculation flow through the fuel elements: 15.8×10^6 lb/h;
- d) output: 506.3 MWt.

In establishing the thermal-hydraulic conditions in the core, allowance was made for crud formation on the fuel elements.

The duration of the cycle was found to be on the order of 2800 MWD/MTU. Fig. 6.5 shows the average burn-up distribution calculated for the end of Cycle 1C.

7. Preparation of the library for the FLARE code

The FLARE code library was integrated with the nuclear constants relating to the three new types of fuel elements which will be inserted in the reactor for the first time at the beginning of Cycle 2 (see paragraphs 3, 4 and 5).

The nuclear constants required for the representation of these elements in the FLARE code were obtained from the results of a series of calculations performed with the BURNY code for each of them. The calculations were used to derive the law of variation of K_{∞} with irradiation at different void contents, with power (to account for the Doppler effect and presence of xenon), and with control rod insertion. The resulting values were corrected by a factor of 1.008 so that they could be correlated to the ones previously used for the representation of the fuel elements of the first load, the latter values having been obtained with the FORM-THERMOS-PDQ code system corrected by the fast fission factor.

The values of K_{∞} at the beginning of the life of the three types of fuel, in the presence of 0, 1 and 2 control rods at rated power and 25% void content are tabulated below:

Type of element	No rods	1 rod	2 rods
Standard UO_2 - PuO_2	1.2592	1.1104	0.9290
Advanced UO_2 - PuO_2	1.2590	1.0949	0.9110
2.3% UO_2	1.2490	1.0751	0.8806

Fig. 6.6 gives the variation of K_{∞} as a function of irradiation for the three types of fuel at rated power and 25% void content; Fig. 6.7 gives the variation of K_{∞} as a function of void content, at rated power and at the beginning of fuel life.

Again with the BURNY code, the values of M^2 as a function of the void content, and ν as a function of burn-up were obtained.

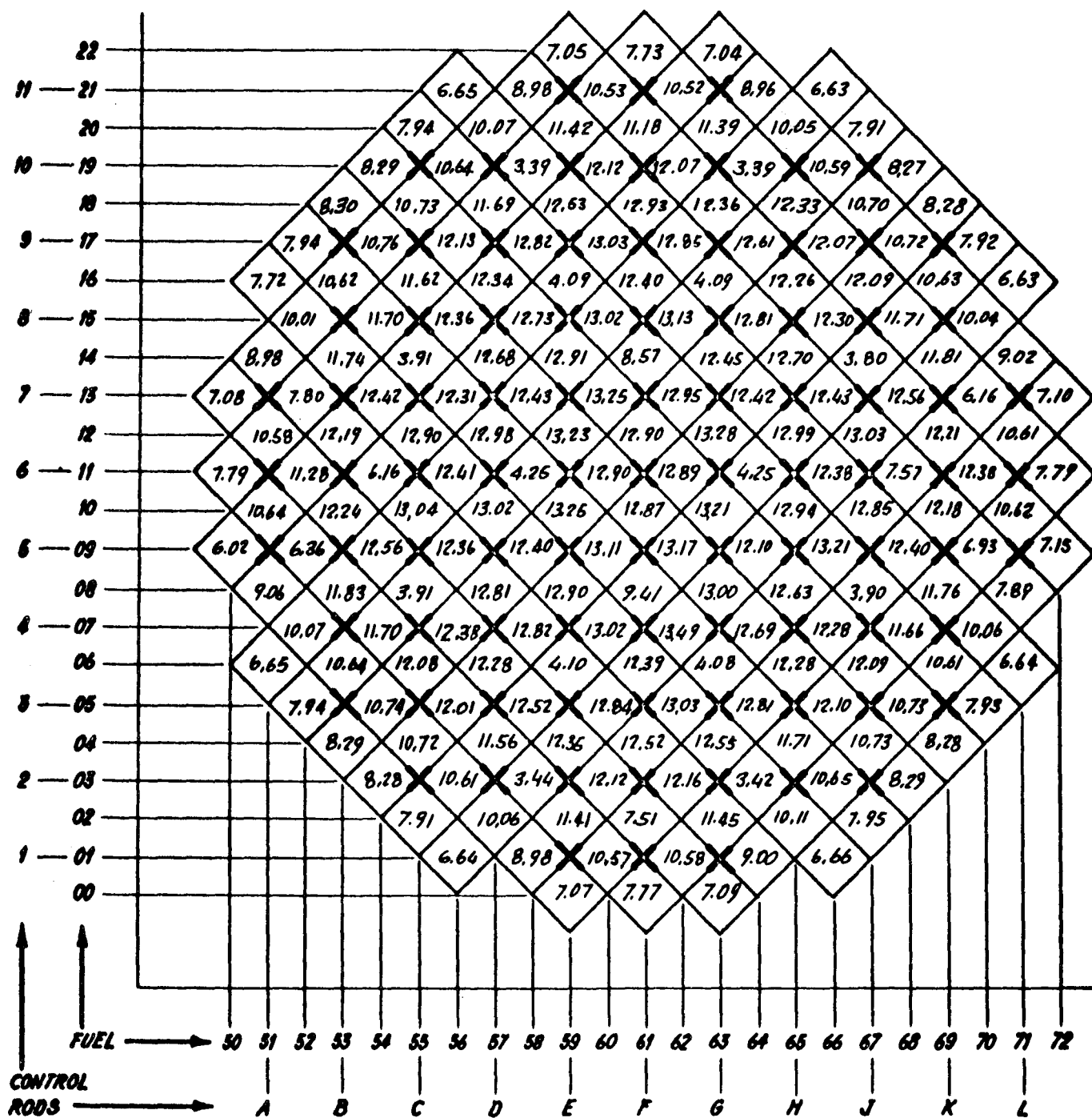


FIG. 6-5-CICLE IC: FINAL DISTRIBUTION OF AVERAGE BURNUP LEVELS (10^3 MWD/MTU)

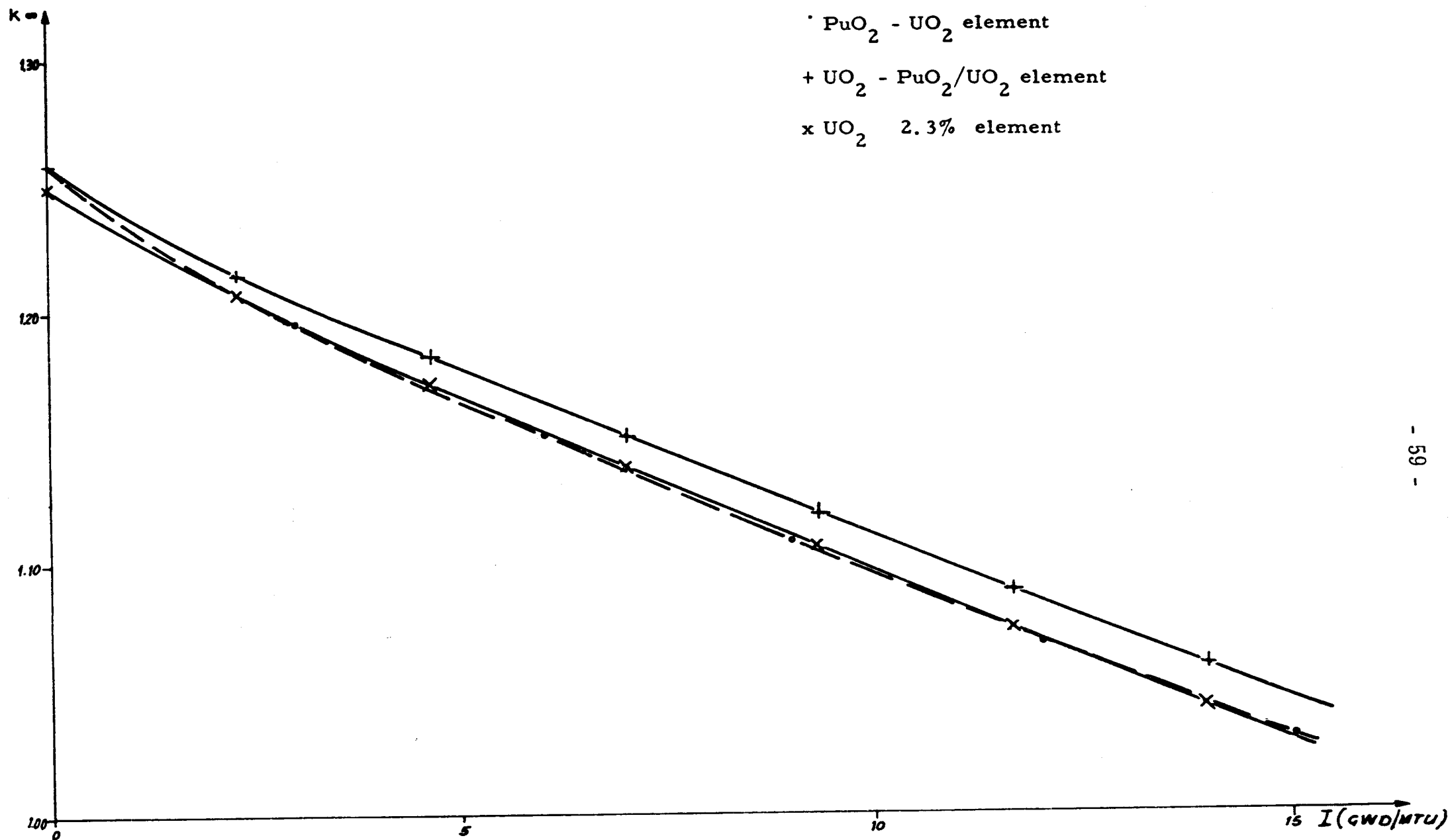


FIG. 6-6 - K_{∞} VERSUS IRRADIATION

TO

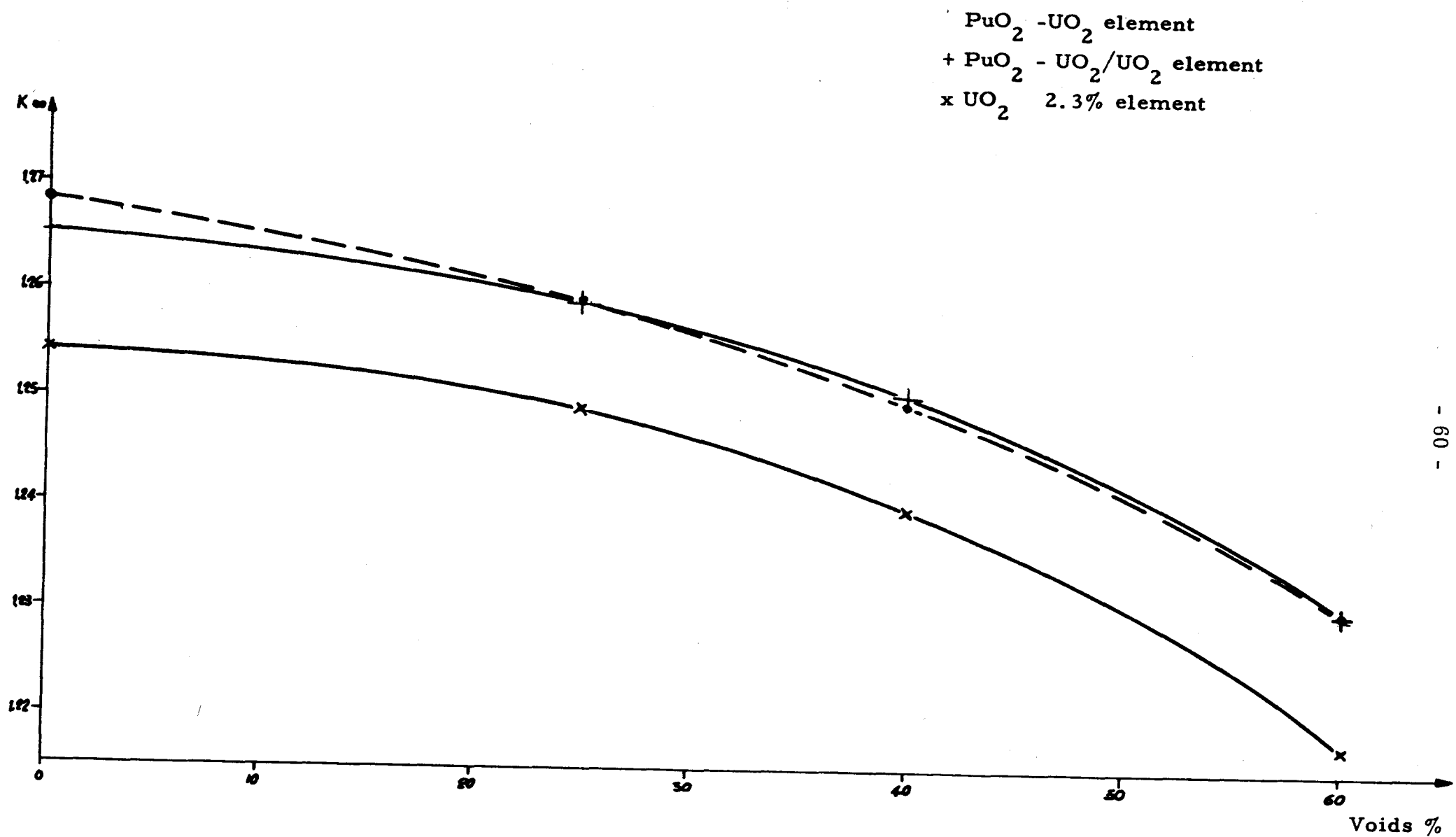


FIG. 6-7 - K_{∞} VERSUS VOID CONTENT

8. Positioning of prototype plutonium elements

The subsequent studies concerned the positions to be given to the twelve plutonium elements in the Garigliano core when they will be inserted at the beginning of Cycle 1. For this purpose, an investigation was carried out with the FLARE code, on the tentative assumption of adopting the pattern shown in Fig. 6.8. The positions of the twelve plutonium elements were selected on the basis of the criteria formulated in paragraph 6.1.

The fourteen fresh elements loaded at the beginning of Cycle 1C were moved to other positions so that they would not be near the elements of the first reload. In fact, the burn-up that these elements will reach at the end of Cycle 1C is rather low (3500 MWD/MTU), and it was thus considered preferable to place them in a checkerboard pattern around the core periphery.

In order to render more evident any possible effects caused to the core power distribution by the presence of the twelve plutonium elements, two calculations were performed; the first was based on a fuel load in which all 66 fresh elements were enriched-uranium; the second considered 54 enriched-uranium and 12 plutonium elements, as shown in Fig. 6.8.

The radial peak factor was calculated on the assumption that the control rods are withdrawn so as to maintain the macroscopic power distribution constant throughout Cycle 2 (Haling technique).

Fig. 6.9 gives the relation between bundle power densities for the two cases described above. From this figure it will be noted that, from the point of view of the average bundle power distribution, there is no substantial difference between a plutonium element and an equivalent enriched-uranium element. The maximum radial peaking factor is increased by about 1% in the case of mixed loads.

9. Analysis of the perturbations in the local power distribution caused by lack of one rod in the reload fuel elements

To further verify the adequacy of the calculation methods, a series of rod power distribution measurements will be performed on activated elements in a critical assembly of 3x3 reload elements. Since the gamma scans will be performed on the individual rods of purposely disassembled elements and this handling may cause the rods to be damaged, a study was carried out to investigate the magnitude of the perturbations caused in the local power distribution by the lack of one rod, just in case the latter should have to be discarded after gamma scanning for the above reason. This investigation was carried out on all three types of reload fuel on the assumption that any type of rod may be missing. Consideration was also given to the advisability of shuffling the rods of one type so as to

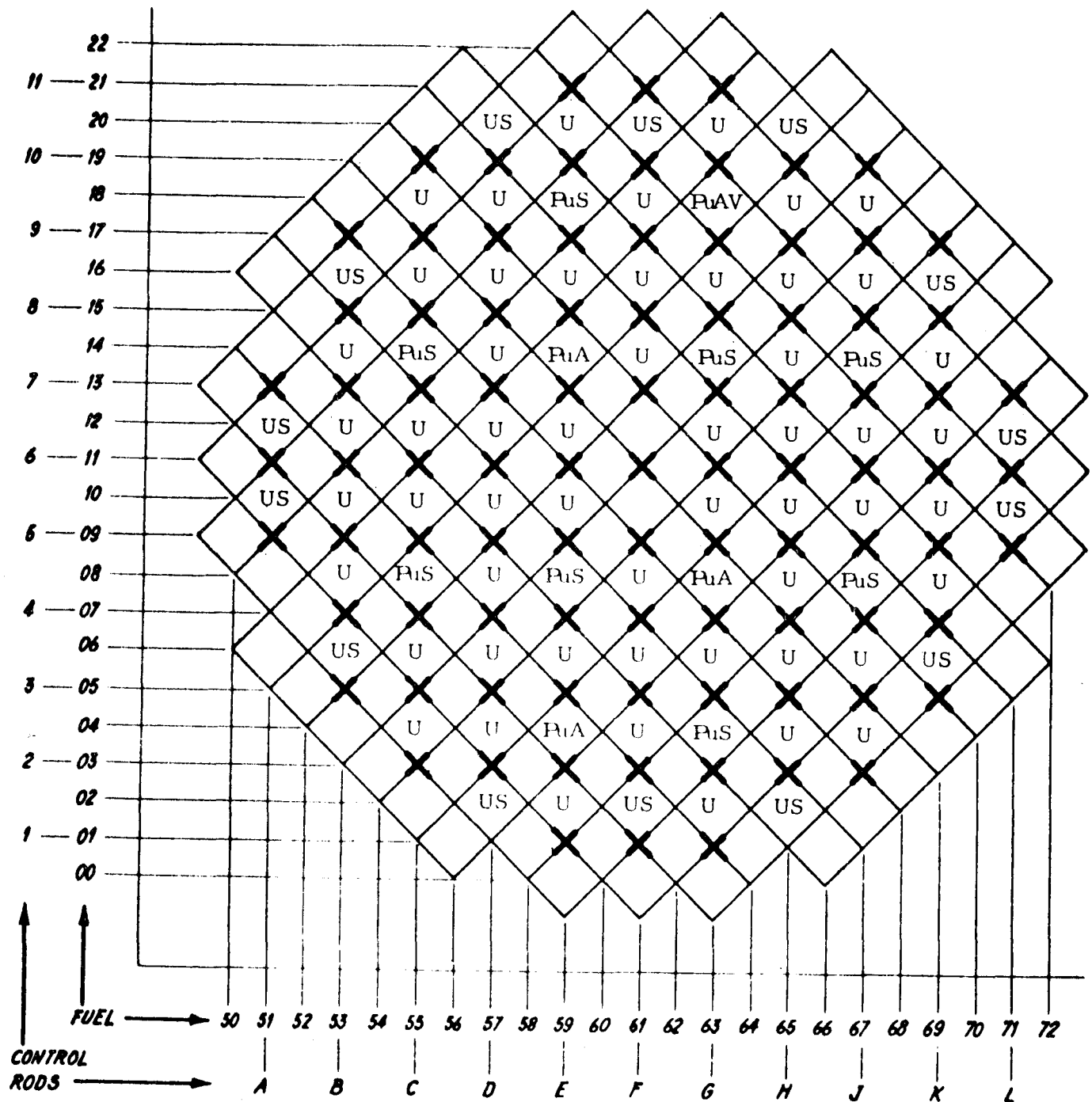


FIG. 6-8 - CYCLE 2: PRELIMINARY LOADING MAP

PuS = "standard" plutonium elements (8)

PuA = "advanced" plutonium elements (3)

PuAV = "vipact advanced"

U = 2.3% U²³⁵ enriched elements (54)

US = 2.02% U²³⁵ enriched elements loaded at beginning of cycle 1C (14)

* Maximum power density location

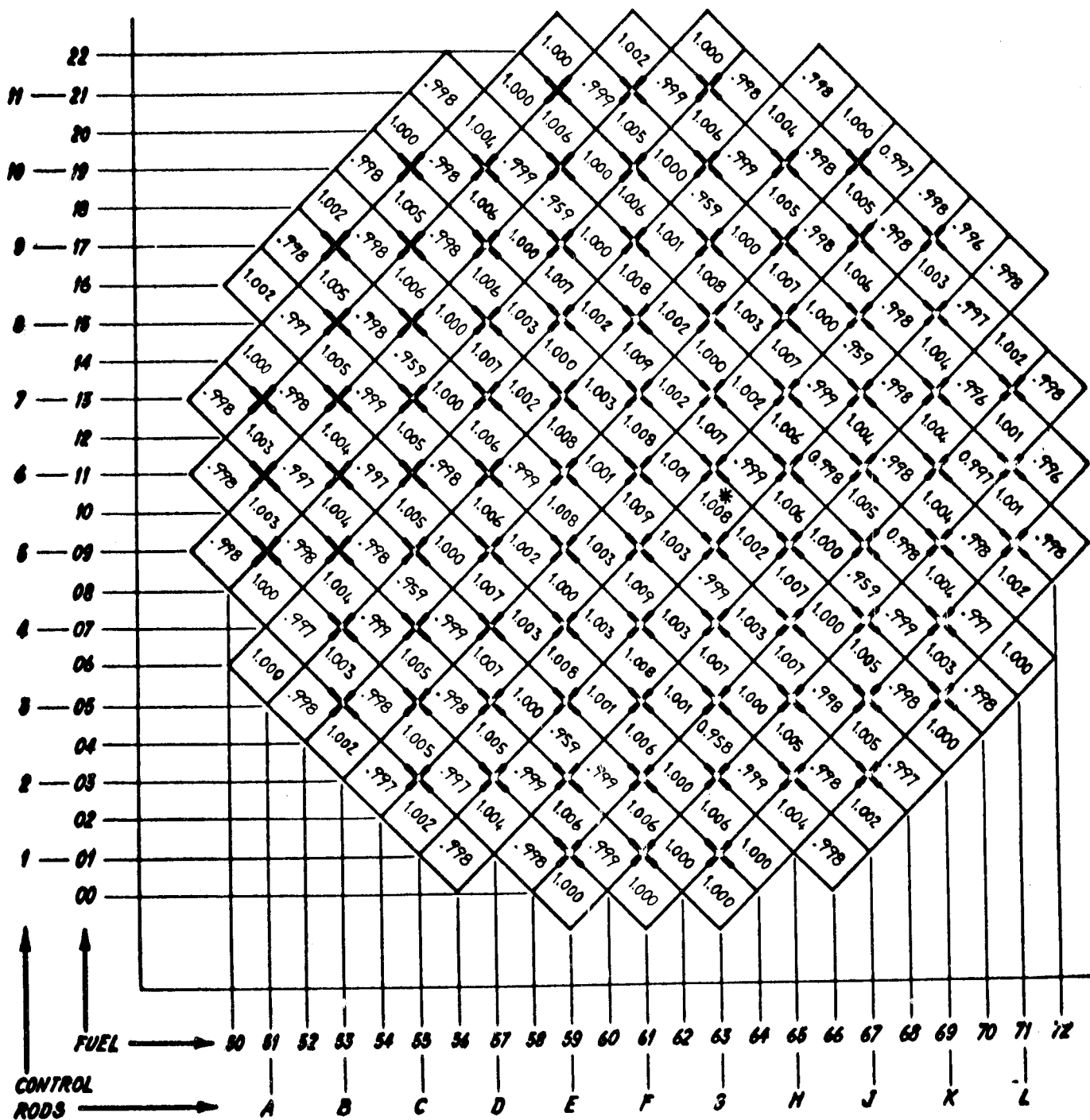


FIG. 6-9 - RELATION BETWEEN BUNDLE POWER DENSITIES FOR MIXED LOADING (54 U^{235} ENRICHED AND 12 PLUTONIUM ELEMENTS) AND UNIFORM LOADING (66 J^{235} ENRICHED ELEMENTS)

locate the water gap in a position where it will affect power distribution less.

The magnitude of this perturbation is shown in Figs 6.10, 6.11, 6.12 for the three types of fuel elements.

The increase in maximum peaking factor is appreciable -- on the order of 5-6% -- when one of the following rods is missing:

Standard plutonium element:	a) 0.74% Pu-enriched rod
	b) 1.40 Pu-enriched rod
Advanced plutonium element:	a) 2.41% U-enriched rod
	b) 1.89% Pu-enriched rod
Uranium reload element:	a) rod enriched to 1.83% in U-235.

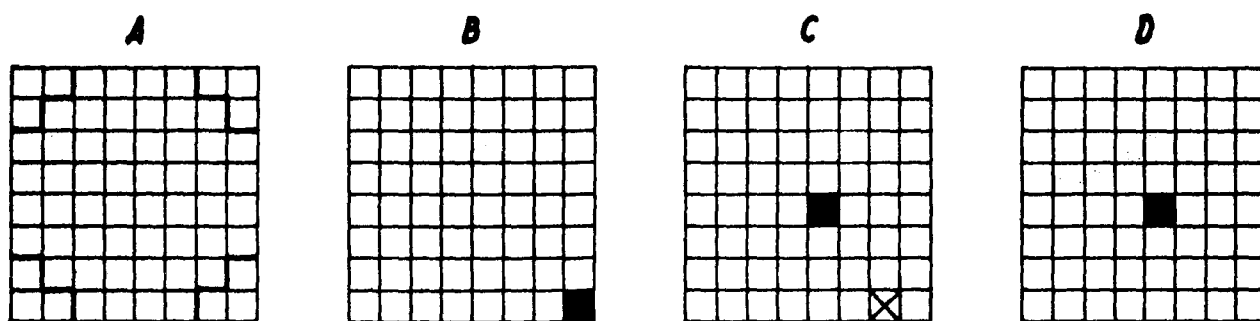
In the other cases, the maximum peaking factor rose negligibly or even decreased.

In addition to the factor due to water gap perturbation (1.05-1.06), another factor of 1.015 must be added to account for the fact that the power is now generated by 63 rods, assuming that the output is the same.

A supplementary analysis indicated that the insertion of an empty Zircaloy tube in the water gap reduces the perturbation factor from 1.06 to 1.03 (Fig. 6.11, case E). This figure also shows that as irradiation increases the perturbation factor decreases gradually till it becomes negligible at about 12,000 MWD/MTU.

Although the insertion of an empty Zircaloy tube improves the power distribution and especially the hydraulic conditions inside the element, an empty cell in the lattice is still acceptable.

Another study was conducted with reference to the standard plutonium element in order to determine how the perturbation changes with irradiation. The results are indicated in Figs 6.13 and 6.14.



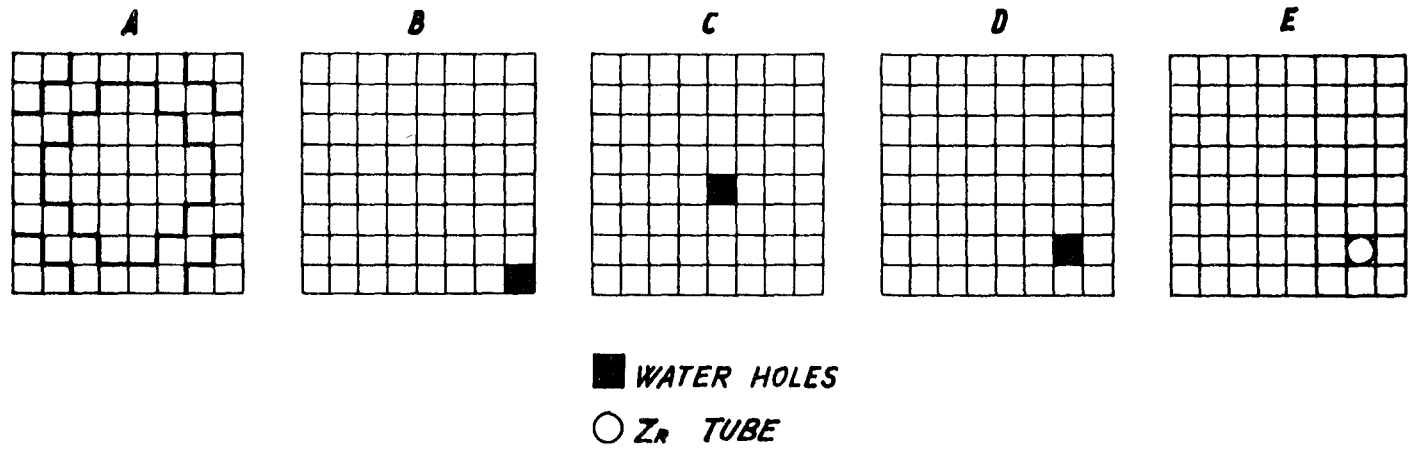
■ WATER HOLES ⊗ 2,3% U^{235}

1.181 1.168 1.156 1.158							1.181 1.167 1.168 1.160
	1.067 1.052 1.046 1.049					1.067 1.055 1.050 1.052	
		.870 .860 .862 .864			.870 .863 .872 .874		
			.801 .793 .830 .832	.801 .795 .858 .860			
			.801 .795 .858 .860	.801 .799 — —			
		.870 .863 .872 .874		.855 .839 .891 .895	.870 .889 .897 .902		
	1.067 1.065 1.050 1.052			.924 .936 .927 .932	.964 1.004 .956 .967	1.067 1.163 1.046 1.059	
1.181 1.167 1.157 1.160				1.124 1.145 1.106 1.114	1.170 1.237* 1.142 1.158	1.025 1.161 1.237* 1.012	1.181* — 1.168 1.163*

A
B
C
D

* Maximum power density rod

FIG. 6-10 - URANIUM RELOAD ELEMENT - PERTURBATION IN THE LOCAL POWER DISTRIBUTION BY LACK OF ONE ROD AT $I = 0$

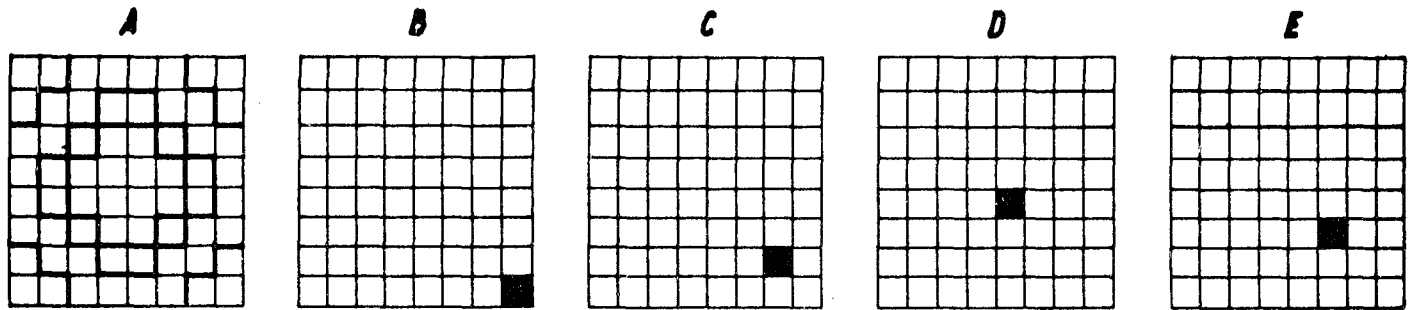


1.219							1.219
1.200							1.201
1.191							1.194
1.193							1.196
1.202							1.204
	1.030					1.030	
	1.018					1.015	
	1.007					1.010	
	1.008					1.011	
	1.016					1.018	
		.958			.958		
		.944			.946		
		.944			.956		
		.939			.942		
		.946			.948		
			.769	.769			
			.767	.758			
			.818	.888			
			.754	.757			
			.759	.751			
			.769	.769			
			.758	.761			
			.888	—			
			.757	.764			
			.761	.767			
		.958		.840	.958		
		.946		.839	.982		
		.956		.958	1.007		
		.942		.851	1.042		
		.948		.850	1.029		
	1.030			1.079	.818	1.030	
	1.015			1.092	.865	1.168	
	1.010			1.081	.814	1.014	
	1.011			1.107	.936	—	
	1.018			1.100	.908	—	
1.219				1.098	1.203	.974	1.219 *
1.201				1.120	1.296 *	1.162	—
1.194				1.079	1.182	.956	1.194 *
1.196				1.114	1.283	1.084	1.299 *
1.204				1.108	1.253	1.032	1.257 *

A
B
C
D
E

* Maximum power density rod

FIG. 6-11 - STANDARD PLUTONIUM ELEMENT - PERTURBATION
IN THE LOCAL POWER DISTRIBUTION BY LACK OF
ONE ROD AT I = 0



■ WATER HOLES

1.142 1.125 1.120 1.116 1.118							1.142 1.127 1.123 1.118 1.121
	.959 .946 .942 .939 .941					.959 .949 .945 .942 .943	
		1.005 .994 .990 .992 .983			1.005 .997 .994 1.002 .989		
			.864 .852 .849 .914 .848	.864 .854 .852 .990 .862			
			.864 .854 .852 .990 .862	.864 .859 .861 — .921			
		1.005 .997 .994 1.002 .989		1.062 1.059 1.070 1.181 * 1.197	1.005 1.038 1.075 1.048 —		
	.959 .949 .945 .942 .943			1.162 * 1.181 * 1.190 1.161 1.220 *	.786 .824 .858 .782 .868	.959 1.052 — .947 1.010	
1.142 1.127 1.123 1.118 1.121				.983 1.003 .998 .967 .990	1.065 1.130 1.121 1.048 1.085	.970 1.104 1.054 .955 .983	1.142 — 1.208 * 1.120 1.145

A
B
C
D
E

* Maximum power density rod

FIG. 6 - 12 - ADVANCED PLUTONIUM ELEMENT - PERTURBATION
IN THE LOCAL POWER DISTRIBUTION BY LACK OF
ONE ROD AT I = 0

I = 3011 MWD/MTU

1.116							1.116
1.100							1.101
1.096							1.094
	1.030					1.030	
	1.015					1.017	
	1.008					1.011	
		.997			.997		
		.984			.986		
		.984			.995		
			.802	.802			
			.790	.792			
			.850	.915			
			.802	.802			
			.792	.795			
			.915	—			
		.997		.877	.997		
		.986		.879	1.026		
		.995		.989	1.044		
	1.030			1.117	.846	1.030	
	1.017			1.134	.892	1.142	
	1.011			1.113	.841	1.015	
1.116				1.077	1.161*	.950	1.116
1.101				1.097	1.233*	1.078	—
1.094				1.059	1.141*	.933	1.095

I = 6022 MWD/MTU

1.034							1.034
1.020							1.021
1.013							1.015
	1.021					1.021	
	1.008					1.010	
	1.001					1.003	
		1.038			1.038		
		1.026			1.029		
		1.025			1.037		
			.838	.838			
			.827	.829			
			.885	.946			
			.838	.838			
			.829	.833			
			.946	—			
		1.038		.919	1.038		
		1.029		.925	1.071		
		1.037		1.024	1.083		
	1.021			1.153*	.871	1.021	
	1.010			1.176*	.975	1.106	
	1.003			1.157*	.867	1.008	
1.034				1.051	1.112	.926	1.034
1.021				1.068	1.164	1.009	—
1.015				1.035	1.095	.910	1.016

I = 12043 MWD/MTU

.944							.944
.934							.935
.928							.928
	.985					.985	
	.975					.976	
	.969					.970	
		1.107			1.107		
		1.096			1.100		
		1.096			1.107		
			.917	.917			
			.908	.911			
			.962	1.010			
			.917	.917			
			.911	.917			
			1.010	—			
		1.107		1.004	1.107		
		1.100		1.016	1.142		
		1.107		1.090	1.145		
	.985			1.200*	.906	.985	
	.976			1.221*	.938	1.023	
	.970			1.204*	.903	.975	
.944				.997	1.022	.895	.944
.935				1.006	1.042	.934	—
.928				.985	1.009	.882	.930

I = 15054 MWD/MTU

.926							
.917							
.911							
	.966						
	.957						
	.951						
		1.129					
		1.119					
		1.120					
			.958	.958			
			.951	.954			
			1.002	1.041			
			.958	.958			
			.954	.961			
			1.041	—			
		1.129		1.042	1.129		
		1.123		1.056	1.159		
		1.130		1.116	1.162		
	.966			1.202*	.916	.966	
	.958			1.220*	.939	.989	
	.953			1.207*	.913	.957	
.926				.975	.988	.888	.926
.918				.980	1.001	.919	—
.912				.965	.977	.876	.913

A
B
C

* Maximum power density rod

Letters refer to cases shown in fig. 6-11

6-13 - STANDARD PLUTONIUM ELEMENT - PERTURBATION LOCAL POWER DISTRIBUTION BY LACK OF ONE ROD VERSUS IRRADIATION

I-3011 MWD/MTU

I-6022 MWD/MTU

1.116							1.116
1.096							1.098
1.102							1.104
	1.030					1.030	
	1.011					1.013	
	1.017					1.019	
		.997			.997		
		.980			.983		
		.986			.989		
			.802	.802			
			.788	.791			
			.793	.795			
			.802	.802			
			.791	.799			
			.795	.801			
		.997		.877	.997		
		.983		.892	1.081		
		.989		.890	1.069		
	1.030			1.117	.846	1.030	
	1.013			1.149	.950	—	
	1.019			1.141	.926	—	
1.116				1.077	1.161*	.950	1.116
1.098				1.093	1.227*	1.033	1.173
1.104				1.086	1.201*	.994	1.160

1.034							1.034
1.017							1.019
1.022							1.023
	1.021					1.021	
	1.005					1.007	
	1.010					1.012	
		1.038			1.038		
		1.022			1.026		
		1.028			1.031		
			.838	.838			
			.825	.828			
			.829	.832			
			.838	.838			
			.828	.837			
			.832	.839			
		1.038		.919	1.038		
		1.026		.938	1.121		
		1.031		.935	1.109		
	1.021			1.155*	.871	1.021	
	1.007			1.190*	.959	—	
	1.012			1.180*	.939	—	
1.034				1.051	1.112	.926	1.034
1.019				1.066	1.162	.987	1.074
1.023				1.060	1.142	.958	1.052

I-12043 MWD/MTU

I-15054 MWD/MTU

.944							.944
.932							.933
.936							.936
	.985					.985	
	.973					.975	
	.976					.978	
		1.107			1.107		
		1.094			1.099		
		1.099			1.102		
			.917	.917			
			.907	.912			
			.911	.914			
			.917	.917			
			.912	.923			
			.914	.923			
		1.107		1.004	1.107		
		1.099		1.029	1.174		
		1.102		1.024	1.163		
	.985			1.200*	.906	.985	
	.975			1.232*	.956	—	
	.978			1.223*	.945	—	
.944				.997	1.022	.895	.944
.933				1.007	1.043	.927	.966
.936				1.002	1.034	.911	.953

.926							.926
.916							.917
.919							.919
	.966					.966	
	.955					.957	
	.958					.959	
		1.129			1.129		
		1.117			1.122		
		1.121			1.125		
			.958	.958			
			.950	.955			
			.953	.957			
			.958	.958			
			.956	.967			
			.957	.966			
		1.129		1.042	1.129		
		1.122		1.068	1.181		
		1.125		1.063	1.172		
	.966			1.202*	.915	.966	
	.957			1.227*	.949	—	
	.959			1.220*	.941	—	
.926				.975	.988	.888	.926
.917				.981	1.002	.916	.945
.919				.978	.995	.900	.934

A
D
E

* Maximum power density rod

Letters refer to cases shown in fig. 6-11

FIG. 16-14 - STANDARD PLUTONIUM ELEMENT - PERTURBATION LOCAL POWER DISTRIBUTION BY LACK OF ONE ROD VERSUS IRRADIATION

TASK VII - REACTOR SAFETY ANALYSIS. PLANT BEHAVIOUR
DURING OPERATING TRANSIENTS AND ACCIDENTS

The work under this task was limited to the health physics problems associated with plutonium fuel handling. For the various operations on the fuel, including rod gamma scanning, it was necessary to set the handling procedures and to have adequate supervisory instrumentation such as would provide maximum safety for the personnel and permit periodical exposure checks.

It should be pointed out that the handling of the Garigliano plutonium elements does not give rise to particular radiological problems, because both the plutonium concentration and the Pu-241 content are low (less than 2% and about 1%, respectively). Measurements taken on the surface of newly fabricated rods gave dose values of only a few mrem/h.

Supervision of the handling operations and periodical personnel checks require:

- (1) a check for surface contamination of the fresh elements (source contamination);
- (2) a check for surface contamination in the event of accidental fall and consequent breakage of a fuel rod;
- (3) a routine check of the room activity;
- (4) laboratory analyses of the personnel's organic liquids in case of rupture of fuel elements.

Surface contamination under 1 above will be monitored through laboratory analyses of swabs. The analyses will first determine the total alpha activity and then the contribution by plutonium to that activity.

The measurement of surface contamination under 2 will be taken directly in situ with portable alpha counters. If necessary, more detailed analyses will be performed on swabs as in 1 above.

For the determination of room activity, samples of airborne dust collected on suction filters will be analyzed.

With regard to the remote probability of a fuel rod being dropped accidentally during handling, it should be borne in mind that this operation is carried out only inside the containment sphere which can be isolated and evacuated.

The Health Physics team will provide for all necessary checks and decontamination of areas, if necessary.

Supplementary instrumentation was needed for:

- shipment, handling and loading of fresh fuel elements;
- irradiation during the minimum critical experiment;
- disassembly of the element, after the minimum critical measurements, for gamma scanning of the individual rods.

Since most of the instrumentation required for these purposes was already available, the procurements was limited to alpha-counters and gamma spectrometers.

TASK VIII - CONCEPTUAL MECHANICAL DESIGN OF THE FUEL
ELEMENT AND TECHNICAL SPECIFICATIONS FOR
FUEL PROCUREMENT

In the course of a meeting in Brussels on 19-21 September 1967, detailed discussions were held with Community manufacturers on the main problems associated with the fabrication of a second series of four prototype elements so that the manufacturers' particular requirements could be taken into account in writing the technical specifications.

The discussions with the manufacturers led to the definition of the following main points:

1. The fuel was to be constituted of pellets of mixed uranium and plutonium oxides. Other fabrication techniques could be submitted as alternatives.
2. The mechanical and thermal-hydraulic design of the elements would be under the manufacturer's sole responsibility, whereas ENEL would prepare the nuclear design.
3. The average plutonium content in the element would be about 1.8w/o. ENEL would specify the final value of plutonium content not later than ten months prior to delivery and after having taken cognizance of the details of the mechanical design.
4. The supplier would be responsible for the procurement of all materials except plutonium.
5. Plutonium would be delivered to the supplier eleven months prior to the fuel element delivery date in the form of oxide. The anticipated isotopic composition was:

Pu-239	82%
Pu-240	14%
Pu-241	3%
Pu-242	1%

6. The elements were to be designed to operate on a continuous basis at a linear power density around 500 W/cm².
7. The elements would be designed for an average burnup of about 25,000 MWD/MT (U+Pu).
8. The specifications for the inspections and quality control would be prepared by the supplier on the basis of an outline provided by ENEL.

ENEL sent out enquiries in January 1968. The technical and economic analysis of the bids received is still under way.

LIST OF REPORTS ISSUED DURING THE SECOND YEAR OF IM-
PLEMENTATION OF THE ENEL-EURATOM CONTRACT 092-66-6-TEEI

1. Risultati dei lavori effettuati dal 1 giugno 1966 al 31 maggio 1967.
Relazione annuale n. 1. Doc. 4.811/7
2. Risultati dei lavori effettuati dal 1 aprile al 30 giugno 1967. Rela-
zione trimestrale n. 4. Doc. 4811/8.
3. Risultati dei lavori effettuati dal 1 luglio al 30 settembre 1967. Re-
lazione trimestrale n. 5. Doc. 4.811/9.
4. Risultati dei lavori effettuati dal 1 ottobre al 31 dicembre 1967. Re-
lazione trimestrale n. 6. Doc. 4.811/10.
5. Risultati dei lavori effettuati dal 1 gennaio al 31 marzo 1968. Rela-
zione trimestrale n. 7. Doc. 4.811/11.



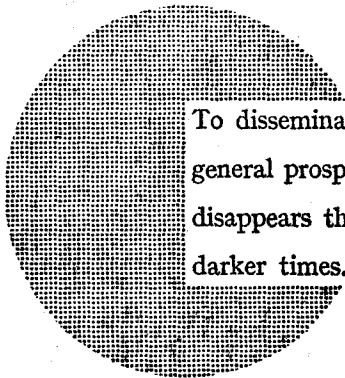
NOTICE TO THE READER

All Euratom reports are announced, as and when they are issued, in the monthly periodical **EURATOM INFORMATION**, edited by the Centre for Information and Documentation (CID). For subscription (1 year : US\$ 15, £ 6.5) or free specimen copies please write to :

Handelsblatt GmbH
"Euratom Information"
Postfach 1102
D-4 Düsseldorf (Germany)

or

Centrale de vente des publications
des Communautés européennes
37, rue Glesener
Luxembourg



To disseminate knowledge is to disseminate prosperity — I mean general prosperity and not individual riches — and with prosperity disappears the greater part of the evil which is our heritage from darker times.

Alfred Nobel

SALES OFFICES

All Euratom reports are on sale at the offices listed below, at the prices given on the back of the front cover (when ordering, specify clearly the EUR number and the title of the report, which are shown on the front cover).

CENTRALE DE VENTE DES PUBLICATIONS DES COMMUNAUTES EUROPEENNES

37, rue Glesener, Luxembourg (Compte chèque postal N° 191-90)

BELGIQUE — BELGIË

MONITEUR BELGE
40-42, rue de Louvain - Bruxelles
BELGISCH STAATSBLAD
Leuvenseweg 40-42 - Brussel

DEUTSCHLAND

BUNDESANZEIGER
Postfach - Köln 1

FRANCE

SERVICE DE VENTE EN FRANCE
DES PUBLICATIONS DES
COMMUNAUTES EUROPEENNES
26, rue Desaix - Paris 15^e

ITALIA

LIBRERIA DELLO STATO
Piazza G. Verdi, 10 - Roma

LUXEMBOURG

CENTRALE DE VENTE
DES PUBLICATIONS DES
COMMUNAUTES EUROPEENNES
37, rue Glesener - Luxembourg

NEDERLAND

STAATSDRUKKERIJ
Christoffel Plantijnstraat - Den Haag

UNITED KINGDOM

H. M. STATIONERY OFFICE
P. O. Box 569 - London S.E.1

EURATOM — C.I.D.
29, rue Aldringer
L u x e m b o u r g